Two closely related *Arabidopsis thaliana* SNAREs localized in different compartments of *Nicotiana tabacum* secretory pathway

A thesis submitted to the College of Graduate Studies and Research in partial fulfilment of the requirements for the Degree of Master of Science in the Department of Biology

University of Saskatchewan

Saskatoon, Saskatchewan

By Marika Rossi

PERMISSION TO USE

In presenting this thesis in partial fulfilment of the requirements for a Postgraduate degree from the University of Saskatchewan, I agree that the Libraries of this University may make it freely available for inspection. I further agree that permission for copying of this thesis in any manner, in whole or in part, for scholarly purposes may be granted by the professor or professors who supervised my thesis work or, in their absence, by the Head of the Department or the Dean of the College in which my thesis work was done. It is understood that any copying or publication or use of this thesis parts thereof for financial gain shall not be allowed without my written permission. It is also understood that due recognition shall be given to me and to the University of Saskatchewan in any scholarly use which may be made of any material in my thesis.

Requests for permission to copy or to make other use of material in this thesis in whole or part should be addressed to:

Head of Department of Biology

University of Saskatchewan

Saskatoon, Saskatchewan S7N 5E2

Canada

ABSTRACT

The secretory pathway of plant cells consists of several organelles that are connected by vesicle and tubular transport. Every compartment has a distinct function and the specificity of vesicle fusion is essential to maintain the organelle's identity. N-ethylmaleimide-sensitive factor attachment protein receptors (SNAREs) play a crucial role in the secretory pathway driving specific vesicle fusions. A vesicle SNARE (v-SNARE) on a vesicle specifically interacts with two or three target SNAREs (t-SNAREs) on the target compartment. This event leads to vesicle membrane fusion with the membrane of the target compartment and the release of cargo molecules into the organelle lumen.

The aim of this work was the characterization of two *Arabidopsis thaliana* SNAREs. The first one is a v-SNARE, Bet11 that is the Arabidopsis ortholog of the yeast and mammal ER-Golgi v-SNARE, Bet1. In these organisms, Bet1 is involved in trafficking between the ER and Golgi apparatus. The second protein studied is a putative SNARE called Bet12 that shares high sequence identity with Bet11. In particular, I was interested in studying the sorting of these two proteins and their role in the secretory pathway of plant cells. By confocal laser microscopy, I demonstrated that these two proteins have different intracellular localization: Bet11 was mainly localized on the ER, Golgi stacks and punctate structures that I have identified as endosomes. Bet12 was localized only on the Golgi stacks. The identification of signal(s) involved in targeting of Bet11 and Bet12 were studied. To reach this aim I generated different mutant chimeras of Bet11 and Bet12. The co-expression of these chimeras with specific protein markers suggested that the distribution of these proteins was the result of a combined influence of multiple domains.

A serine in the Bet11 sequence was identified as a putative phosphorylation site and appeared important for proper Bet11 intracellular distribution.

The different intracellular distributions of Bet11 and Bet12 suggest different biological roles for the two proteins. To functionally characterize these two proteins homozygous knock-down mutants of Bet11 were screened. These plants had no evident phenotype, suggesting a possible genetic redundancy in this SNARE family.

ACKNOWLEDGEMENTS

I am deeply grateful to my supervisor Professor Federica Brandizzi for her expertise and her strong passion for science that have been an example to follow. Her encouraging and personal guidance have been determinant during these years.

I would like to thank my committee members Professor Peta Bonham-Smith and Dr Jonathan Page for their advice and constructive comments.

I am sincerely grateful to Professor Jurgen Denecke for hosting me in his lab, for his wide knowledge and kind support.

I would like to thank my colleagues in the lab for their collaboration and help. In particular I am sincerely grateful to Dr. Loren A. Matheson for revising the English of this manuscript, Dr. Laurent Chatre for cloning Bet11 and Bet12 and for his crucial bioinformatic and intellectual contribute to sequence alignments. A special thank goes to Luciana Renna and Giovanni Stefano for their precious support and friendship.

I would like to express my gratitude to the University of Saskatchewan Department of Biology, to the University of Leeds Department of Biology and to the Michigan State University Plant Research Laboratory.

I owe my warm thanks to my family and friends for their support. My loving thanks are due to Carlo Cravero for his encouraging patience and help.

TABLE OF CONTENTS

LIST OF FIGURES

LIST OF TABLES

LIST OF ABBREVIATIONS

Bet	Block Early in Transport
CCV	Clathrin Coated Vesicles
CFP	Cyan Fluorescent Protein
COPI	Coat Protein complex I
COPII	Coat Protein complex II
DV	Dense Vesicle
EE	Early Endosomes
ER	Endoplasmic Reticulum
ERD2	ER-retention defective receptor 2
GFP	Green Fluorescent Protein
LB	Luria Bertani
LE	Late Endosomes
LSCM	Laser Scanning Confocal Microscope
NSF	N-ethylmaleimide-sensitive factor
PM	Plasma Membrane
PVC	Pre-Vacuolar Compartment
RE	Recycling Endosomes
ROS	Reactive Oxygen Species
SNARE	Soluble N-ethylmaleimide-sensitive factor attachment receptors
ST	Sialyltransferase
TGN	Trans-Golgi Network
YFP	Yellow Fluorescent Protein
α-SNAP	*N*-ethylmaleimide-sensitive factor *a*ttachment *p*rotein

1. INTRODUCTION

1.1 The Plant Secretory Pathway

The plant secretory pathway consists of physically separated compartments that continuously exchange membranes and cargo proteins (Jurgens, 2004) (Figure 1.1). Secretory organelles are involved in synthesis, modification, transport and storage of proteins and other macromolecules, such as lipid and carbohydrates (Jurgens, 2004). These compartments are connected by vesicular and tubular transport. The composition and the identity of each organelle depend on a flux of proteins and lipids that they receive and dissipate through an exchange with the cytosol and other organelles (De Matteis and Luini, 2008, Sallese et al., 2006). Such an exchange is maintained by the specificity of shuttling and fusion of vesicles between different secretory compartments (Sallese et al., 2006). The main organelles of the plant secretory pathway are the endoplasmic reticulum (ER), the Golgi stacks, the *trans*-Golgi Network (TGN), the storage and the lytic vacuole, endosomes and the plasma membrane (PM) (Figure 1.1).

1.1.1 Endoplasmic Reticulum

The ER is functionally the first organelle of the secretory pathway. Neo-synthesized proteins that carry the correct targeting determinants enter the ER co- or post-translationally to be eventually secreted or distributed into the membranes or lumen of the different compartments of the endomembrane system (Vitale and Boston, 2008). In the ER lumen the neo-synthesized secretory proteins are folded and modified before

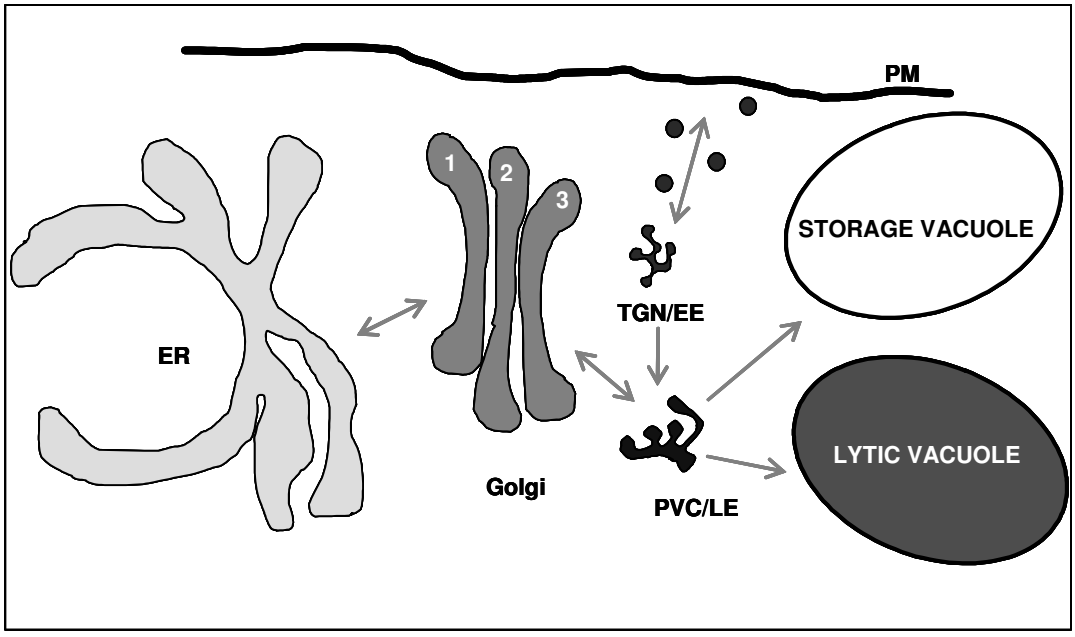

Figure 1.1 Schematic representation of the organelles in the secretory pathway of plant cells. ER = endoplasmic reticulum; 1 = cis- 2 = medial- 3 = trans-Golgi; PVC/LE = prevacuole/late endosome; TGN/EE = trans-Golgi network/early endosome; PM=plasma membrane.

they reach their final destination (Vitale and Boston, 2008). If neo-synthesized proteins are not retained in the ER, they leave this organelle and reach the Golgi stacks. The flow that originates from the ER for protein delivery to the PM or vacuoles via the Golgi stacks is called the *anterograde* pathway. This pathway is counterbalanced by *retrograde* membrane flow that is fundamental for the recycling of molecules involved in the *anterograde* route (Sannerud et al., 2003). The retrograde pathway can be divided into three steps: transport from endocytic compartments to Golgi apparatus, intra-Golgi transport and transport from the Golgi apparatus to the ER (Sannerud et al., 2003).

1.1.2 The Golgi stacks

In mammalian cells, the Golgi apparatus consists of several stacks composed of flat cisternae connected by tubular structures. The entire structure remains clustered in the perinuclear region of a cell by means of a microtubule mechanism (Polishchuk and Mironov, 2004). Plant and yeast cells do not have clustered Golgi apparatus. In the yeast *Pichia pastoris*, only a single Golgi stack is present; whereas in *Saccharomyces cerevisiae*, the Golgi apparatus consists of individual cisternae distributed in the cytoplasm (Nakano, 2004). The plant Golgi apparatus also consists of many stacks of cisternae dispersed in the cytoplasm. These stacks are motile and closely associated with the ER (Hawes et al., 2008; Boevink et al., 1998). (From here I will refer to the plant Golgi as Golgi stacks and to the mammal and yeast Golgi as Golgi apparatus).

The Golgi stacks are generally organized in three morphologically and functionally distinct compartments with a recognizable *cis-trans* polarity: the *cis*-, the *medial*- and the *trans*-Golgi. The *cis* face is closely associated with the ER and exchanges proteins

and membranes with this organelle. The *medial* region is made of tubular and vesicular elements and contains the major enzymes for glyco-protein modifications. Finally, the main role of the *trans*-face is protein sorting to the PM and vacuole (Polishchuk and Mironov, 2004).

The Golgi stacks perform three key functions essential for eukaryotic cell life. First, they act as a "factory" for the modification of proteins and lipids that pass through these compartments, mostly by glycosylation (Altan-Bonnet et al., 2004). Second, the Golgi stacks function as a sorting station of the secretory pathway: from this organelle proteins can be delivered to different destinations (Jurgens, 2004). Finally, the Golgi stacks act as a membrane scaffold onto which different signaling sorting and cytoskeleton proteins adhere (Altan-Bonnet et al., 2004).

1.1.3 *Trans*-Golgi Network and endosomes

The *trans*-Golgi network (TGN) is a complex of tubular membranes that originates from the *trans*- face of the Golgi stacks (De Matteis and Luini, 2008). Essentially, the TGN is the crossroad of the endocytic and exocytic pathways and it is considered the major sorting point of the plant secretory pathway. In fact, different cargo molecules are targeted to several distinct destinations as they pass through the TGN. At this point the sorting machinery controls several pathways directed to distinct compartments such as the PM, endosomes (early, late and recycling) and the PVCs (Lam et al., 2007). At the same time, the TGN acts as an acceptor compartment for endosomal traffic. This retrograde transport is fundamental to recycle sorting proteins belonging to the TGN after their function has been completed (De Matteis and Luini, 2008).

The TGN also has an important biosynthetic function. In fact, in this compartment

many proteins and lipids receive their final post-synthetic modifications such as glycan modification of glycoproteins or completion of lipid synthesis (De Matteis and Luini, 2008).

As mentioned earlier, the TGN is in close association with the endosomal system. In mammalian cells it is possible to distinguish four classes of endosomes: early, late, recycling endosomes and lysosomes (Mellman, 1996). The early endosomes (EE) are tubular/vesicular compartments that exchange materials directly with the PM (Lam et al., 2007). The compartments that receive cargo molecules from the EE are called late endosomes (LE). These deliver cargo molecules to lysosomes where they are degraded. Finally, there are the recycling endosomes (RE), tubular structures that probably act as an intermediate compartment between the TGN and the PM (Lam et al., 2007; De Matteis and Luini, 2008).

Little is known about endosomes in plants and not all endosomal organelles have been well characterized. Nevertheless, Ueda et al. (2004) demonstrated that in *Arabidopsis* protoplasts, two populations of endosomal compartments exist and they have been classified as EE and LE. These authors also confirmed that EE coincide with the TGN and LE and PVC can be considered a unique compartment. Finally, Ueda et al. (2004) noticed a partial overlapping of these two populations of organelles that suggested possible maturation of these compartments from one to the other.

1.2 Vesicular transport in secretory pathway

In eukaryotic cells, the transport of cargo molecules between compartments of the secretory pathway is mediated by vesicles that bud from one membrane and fuse with another (Sallese et al., 2006). Each vesicle transport event can be divided into four steps:

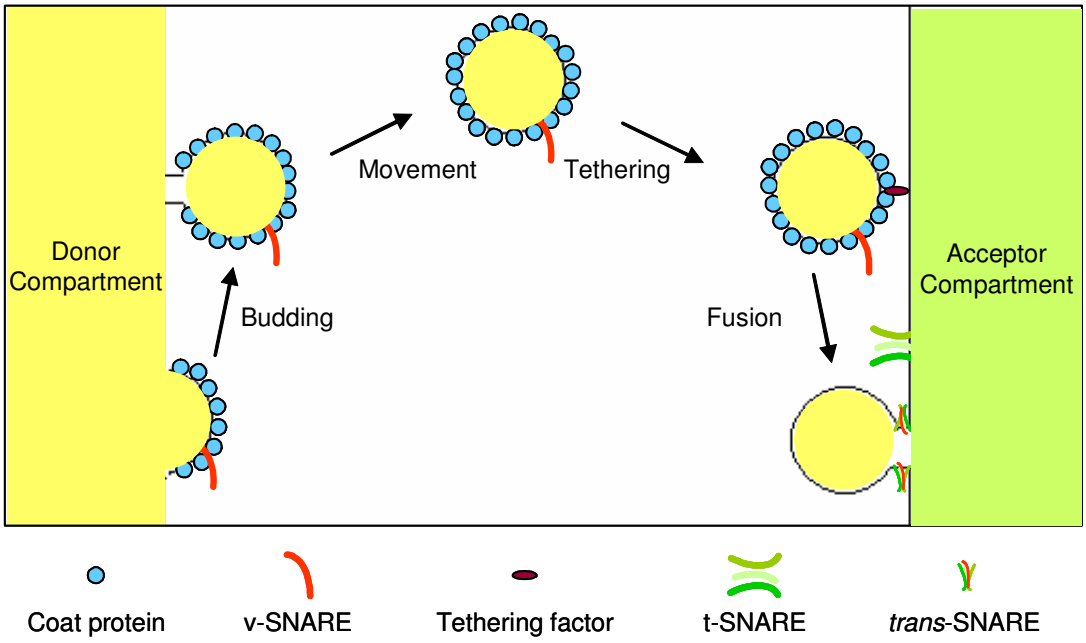

Figure 1.2 Schematic representation of the four essential steps in vesicle transport. Budding is the first step of vesicle formation. Coat proteins are recruited onto the membrane of the donor compartment and this event induces vesicle formation. The v-SNARE interacts with coat proteins and this event leads to the incorporation of the SNARE into the novel vesicle. The vesicle moves into the cytosol toward the acceptor compartment. This movement depends on the interaction with microtubules and actin filaments (Kreft et al. 2009). In proximity of the acceptor compartment tethering factors work to anchor the vesicle to the target membrane. The last step of the vesicle transport is the fusion with the membrane of the target compartment. The interaction between v-SNAREs and the t-SNAREs leads to the formation of a *trans*-SNARE complex. This event provides the required energy to drive membrane fusion. (Figure modified from Bonifacino and Glick, 2004).

vesicle budding, transport, tethering and fusion (Figure 1.2). During "vesicle budding" a vesicle forms on a donor compartment and departs from it. This process is mediated by coat proteins (Cai et al., 2007; Bonifacino and Lippincott-Schwartz, 2003). Coats are complexes of soluble cytosolic proteins that are recruited onto the donor membranes by small GTPases of the Arf1/Sar1 family (Springer et al., 1999).

The major roles of these complexes include deformation of membranes to allow vesicle budding (Antonny et al., 2003) and selection of membrane cargo proteins upon recognition of sorting signals on the cytosolic domains (Mossessova et al., 2003). The sorting signals are sequences or structural motifs that interact with specific recognition factors that determine the trafficking or the localization of the protein. Only the cargo proteins are incorporated in the budding vesicle during a selective process called "cargo sorting" that permits discrimination between cargo and resident proteins.

The different transport steps of the secretory pathway are mediated by coat complexes and sorting signals. Clathrin was the first coat protein to be identified (Pearse, 1975). In yeast and mammalian cells, clathrin coats participate in both exocytic and endocytic vesicular transport (Nakatsu and Ohno, 2003). Recently, it has been proven that clathrin coated vesicles (CCV) are also implicated in plant endocytosis (Dhonukshe et al., 2007). Nevertheless, the role of CCV in the post-Golgi anterograde pathway in plant cells is still not completely understood. However, the detection of a clathrin coat on restricted surface regions of the *trans*-Golgi suggested the possible involvement of CCV in vacuolar transport (Otegui et al., 2006). In mammals and yeast, subsequent studies have identified two non-clathrin coats: coat protein complex I (COPI) and coat protein complex II (COPII) that are involved in vesicular transport between the ER and Golgi stacks. COPII is the protein coat complex involved in the formation of vesicles that

transit from the ER to the Golgi stacks (Barlowe et al., 1995; Matheson et al., 2006; Paul and Frigerio, 2007). The COPII complex is well understood in mammals and yeast and most proteins of the COPII complex have also been studied in plants (da Silva et al., 2004; Stefano et al., 2006b; Hanton et al., 2007; Hanton et al., 2008; Hanton et al., 2009). Retrograde transport from the Golgi stacks to the ER and the transport of Golgi stack resident proteins between cisternae are driven by the COPI complex (Letourneur et al., 1994; Hanton et al. 2005; Paul and Frigerio, 2007). In addition, it has been demonstrated that not all vesicular traffic is dependent on coat proteins. In some plants, for example, the post-Golgi traffic of storage proteins is dependent on "dense vesicles" (DVs) with no detectable protein coat (Hohl et al., 1996; Robinson et al., 1998). These vesicles are believed to transport storage proteins from the Golgi stacks to the plant storage vacuole (Hohl et al., 1996; Hillmer et al., 2001).

After the budding event, vesicles are transported to their final destination by diffusion or by active transport on the cytoskeleton (Cai et al., 2008). Subsequently, vesicles are targeted to their acceptor compartments. The initial interaction between the vesicle and the target membrane is called tethering. In mammals and yeast, several tethering factors have been identified and they are involved in specificity of vesicle trafficking (Bonifacino and Glick, 2004; Cai et al, 2008). The last step of vesicular mediated transport is the fusion of the vesicle membrane with the target membrane and the release of the cargo into the lumen of the target compartment. In this event, the soluble N-ethylmaleimide-sensitive factor (NSF) attachment protein receptors (SNAREs) are believed to facilitate the fusion of the vesicular membranes to the target compartments (Bonifacino and Glick, 2004).

1.3 SNAREs

SNARE proteins are key elements in membrane fusion in all trafficking steps in the secretory pathway (Jahn and Scheller, 2006). In the *Arabidopsis thaliana* genome, 54 genes coding for SNAREs or putative SNAREs have been identified (Sanderfoot et al. 2000) and many of these genes have high sequence identity with genes of SNAREs from other eukaryotic organisms.

1.3.1 SNARE structure and nomenclature

Structurally, SNAREs have a variable N-terminal domain, a conserved central region and a C-terminal domain involved in membrane anchoring. The N-terminal domain appears to be necessary for membrane fusion (Jahn and Scheller, 2006). The N-terminal domain is connected by a short linker with the conserved central domain called a SNARE-motif. The SNARE-motif is highly conserved between SNAREs. This is a central region of 60-70 amino acids that are arranged in heptad repeats. The SNARE-motif mediates the SNARE-complex formation that drives membrane fusion. Four SNAREs interact to form the SNARE complex. SNARE-motifs, unstructured when the proteins are monomeric, form a four helix bundle and the free energy released during the process of complex formation is used to drive membrane fusion (Jahn and Scheller, 2006).

Most SNAREs have a single C-terminal transmembrane domain. In a few cases, this domain is modified with post-translational modifications, such as palmitoylation, that anchor proteins to membranes (Jahn and Scheller, 2006).

Originally, SNAREs were defined as either a t-SNARE, if localized on the target compartment, or v-SNARE, if associated with the membrane of a vesicle (Söllner et al.,

1993). Subsequently, to avoid ambiguity in the case of homotypic membrane fusion, SNAREs were reclassified as Q- and R-SNAREs according to the presence of a glutamine (Q) or an arginine (R) residue in the central position of the SNARE motif. The role of the amino acids Q and R is still unclear but a high conservation between different organisms suggests a role within the SNARE complex stability. The Q-subfamily can be further subdivided in Qa, Qb and Qc on the basis of sequence identity of the SNARE domain. The SNARE complex formation requires one of each of the Qa, Qb, Qc, and R-SNAREs (Fasshauer et al., 1998).

1.3.2 Localization and sorting

The pool of SNAREs in eukaryotic cells consists of numerous members. *In vitro* tests have demonstrated that a single SNARE may interact either with one specific set of partners or, nonspecifically, with several different partners. This promiscuity is due to the high degree of structural conservation between different SNARE complexes (Jahn and Scheller, 2006). For this reason, sorting mechanisms must exist to guarantee the correct intracellular SNARE distribution.

In plant cells, SNARE sorting signals are unknown and in mammals and yeast only a few examples have been reported. In the simplest case, the target signal is contained entirely within the transmembrane region (Joglekar et al., 2003 Banfield et al., 1994; Watson et al., 2001; Lewis et al., 2000) but some SNAREs may also contain an additional signal within their cytoplasmic region (Weinberger et al., 2005). Recently, it has been demonstrated that mammalian SNARE ykt6 contains its targeting signal in the N-terminal region, which is completely independent of its SNARE motif and transmembrane domain (Hasegawa et al., 2003).

Whether SNAREs are transported individually or as complexes is still unclear; some SNAREs may contain their own target signal, while several SNAREs may be targeted after interaction with other proteins. During the budding of a vesicle, SNAREs enter into the vesicle like other cargo molecules. It has been demonstrated that coat proteins have an important role in recruiting SNAREs into transport vesicles. It is known, for example, that SNAREs that drive membrane fusion between the ER and Golgi apparatus must enter in COPII vesicles (Springer and Schekman, 1998). Recently, a direct interaction has been demonstrated in *S. cerevisiae* between the SNAREs Sed5p, Bet1p and Sec22p and Sec23/Sec24, a heterodimer of the COPII coat (Mossessova et al., 2003).

1.3.3 SNAREs and membrane fusion

The main role of SNAREs in the secretory pathway of eukaryotic cells is to promote membrane fusion (Jahn and Scheller, 2006). To achieve this, an interaction between a v-SNARE on the vesicle and three t-SNAREs on the target compartment is essential (Fasshauer et al., 1998). This interaction leads to the formation of a *trans*-SNARE complex where the SNARE motifs form a four helical bundle (Weber et al., 1998). This event is believed to decrease the distance between two opposite membranes and to release free energy. Both of these events promote membrane fusion (Weber et al., 1998; Jahn and Scheller, 2006). The energy released during the *trans*-SNARE complex formation is most likely used to overcome the energy barrier between the membranes created from negative charges of phospholipids, thus facilitating the fusion (Fasshauer, 2003). After membrane fusion, the *trans*-SNARE complex becomes a *cis*-SNARE complex on the membrane of the target compartment. To allow recycling of v-SNAREs to the membrane of the donor compartment, the *cis*-SNARE complex needs to be

disassembled. Since this complex is extremely stable, a high energy is required to disassemble it. Such energy is provided by a member of the AAA+ family of ATPases called NSF (Bonifacino and Glick, 2004). To bind the *cis*-SNARE complex, NSF uses a cofactor called *N*-ethylmaleimide-sensitive factor *a*ttachment *p*rotein (α-SNAP) (Bonifacino and Glick, 2004; McNew, 2008). Once the *cis*-SNARE complex is disassembled, v-SNAREs are recycled to the donor compartment and the t-SNARE complex is ready for the next round of fusion events (Chen et al., 2001; Jahn and Grubmuller, 2002).

To avoid inappropriate formation of SNARE complexes and to control SNARE activity, several factors, such as members of the Sec1-Munc-18 protein family and synaptotagmins, as well as regulatory reactions influence the action of SNAREs (Lang and Jahn, 2008). After the *cis*-SNARE complex disassembly, for example, v- and t-SNAREs need to be kept separate until the next fusion event. In mammals and yeast, two cytosolic proteins called GATE-16 and LMA-1 bind single SNAREs and keep them separate (Elazar et al., 2003). Similar factors have yet to be identified in plants.

The SNARE activity can also be regulated by post-translational modifications. For example, in yeast and mammals, it has been demonstrated that certain SNAREs can be phosphorylated and this modification influences the binding of SNARE regulators and the SNARE activity (Gerst, 2003; Weinberger et al., 2005).

Phosphorylation is the addition of a phosphate molecule to the R group of an amino acid (usually, in eukaryotic cells, serine, threonine or tyrosine). This modification plays a crucial role in several cellular processes such as signal transduction, enzyme activity regulation, protein degradation and protein-protein interaction (Hunter, 1995; Marash

and Gerst, 2001). The addition of a phosphate group influences the nature of the protein region that becomes polar and extremely hydrophilic. This modification can lead to conformational change in the structure of the protein and alteration of its activity (Dulhanty and Ryordan, 1994; Hunter 1995).

1.3.4 Non-conventional plant SNARE functions

Recently, evidence has suggested that the role of SNAREs may not be limited to vesicle trafficking. SNAREs also have roles in signal transduction by modulating ion channel activities both directly and indirectly (Pratelli et al., 2004; Arien et al., 2003; Cormet-Boyaka et al., 2002; Ji et al., 2002). This is the case of Syp61, a TGN Qc t-SNARE involved in vesicle trafficking to the PVC. Syp61 knockout plants showed altered root morphology and stomatal movements (Zhu et al., 2002). These results suggest a possible role of Syp61 in maintaining the osmotic solute balance in the vacuole and in regulating transport activity of the tonoplast (Pratelli et al., 2004).

SNAREs may also be involved in pathogen resistance. For example, experiments have shown that when mutated, the *Arabidopsis* PM Qa, Syp121, facilitates pathogen penetration of the leaf surface (Collins et al., 2003; Pratelli et al., 2004). This effect seems to be due to the inability of the plant to fuse reactive oxygen species (ROS)-containing vesicles to fuse with the PM, which is normally driven by Syp121 (Collins et al., 2003; Pratelli et al., 2004). During pathogen attacks, ROS are involved through cell-wall modification and signal transduction and the absence of these compounds leads to major pathogen sensitivity (Collins et al., 2003; Pratelli et al, 2004).

It has been demonstrated that SNAREs also have a role in gravitropism. *Arabidopsis* mutant for Syp22 (Qa) and Vti11 (Qb), two SNAREs involved in the trafficking

between the TGN, PVC and vacuole, presented a suppressed gravitropism and altered stem morphology. This phenotype seemed to correlate with an abnormal distribution of amyloplasts and vacuolar fragmentation (Kato et al., 2002).

1.3.5 Block early in transport 1 (Bet1)

Bet1 is a Qc v-SNARE. In mammals, Bet1 is localized on intermediate compartments, between the ER and Golgi apparatus, as well as on the *cis*-Golgi and it cycles between these compartments and the ER (Zangh et al., 1997; Hay et al., 1998). In yeast, Bet1 is essential and temperature-sensitive mutations of *BET1* block secretion and proper localization of proteins in a pre-Golgi compartment (Newman and Ferro-Novick, 1987; Kipnis et al., 2004). Recently, these mutants have been shown to possess cell wall defects due to a blockage in the early secretory pathway of functional proteins involved in cell wall modifications (Kipnis et al., 2004).

In mammals and yeast, Bet1 interacts with three t-SNAREs, Sec22 (R), Bos1 (Qb) and Sed5 (Qa), to form the *trans*-SNARE complex that is required for trafficking from the ER to the Golgi apparatus (Parlati et al, 2000; Zhang et al., 1997; Xu et al., 2000). In yeast, direct interactions between Bet1 and components of COPI and COPII coat complexes have also been described (Rein et al., 2002; Mossesova et al., 2003). It is possible that these interactions influence the intracellular localization of Bet1 and its recycling between the ER and Golgi apparatus. In particular, the signal ^{51}LxxLE^{55} is a determinant for the interaction between Bet1 and sec23/sec24 a subcomplex of yeast COPII and, consequently, for the export of Bet1 from the ER (Bonifacino and Glick, 2004; Mossesova er al., 2003). No signal for recycling Bet1 from the Golgi apparatus has been identified yet, but recently it has been demonstrated that the SNARE motif of

yeast Bet1 is essential for proper targeting of this protein to the Golgi apparatus (Joglekar et al., 2003).

The SNARE-motif of *Arabidopsis* Bet11 (AtBet11; At3g58170) has 30% sequence identity with the SNARE-motif of Bet1 of rat (rBet1) and 25% with the SNARE-motif of Bet1 of *S. cerevisiae* (ScBet1). Bet11 was identified in a complementation screening of the *sft-1* yeast cell line (Tai and Banfield, 2001). SFT-1 is an essential yeast Golgi apparatus v-SNARE that belongs to the same family as Bet1 (Tai and Banfield, 2001). Structurally, Bet11 is a Qc-SNARE, 122 amino acids in length, with a glutamine in the central position of the SNARE motif. In *Arabidopsis* protoplasts, preliminary data show that Bet11 localizes on the *trans*-Golgi compartment (Uemura et al., 2004, Chatre et al., 2005), but there is very little information about intracellular sorting and functions of Bet11 in plants.

Bet12 (At4g14455) is another SNARE of 130 amino acid residues that shares 60% amino acid sequence identity with Bet11 (Figure 1.3), 29% with rBet1 and 18% with ScBet1. There is also very little information about this protein in the literature, with the exception that similar to Bet11, Bet12 complements *sft-1* mutations in yeast (Tai and Banfield, 2001).

Figure 1.3 Bet11 and Bet12 share 60% sequence identity. A) Sequence alignment of ScBet1 and Bet11. B) Sequence alignment of ScBet1 and Bet12. C) Protein sequence alignment of Bet11 and Bet12 shows that these two proteins share high sequence identity, particularly in the SNARE motif (characters in blue). D) Sequence alignment of the C-terminal region of Bet11, Bet12 and ScSed5 shows a conserved serine residue. The sequence alignments were produced using ClustalW2 (http://www.ebi.ac.uk/Tools/clustalw2/index.html) a multiple sequence alignment program. "*" = identical; ":" = conserved substitutions (same amino acid group: small (small + hydrophobic), acidic, basic, hydroxyl + amine + basic) "." = semi-conserved substitutions.

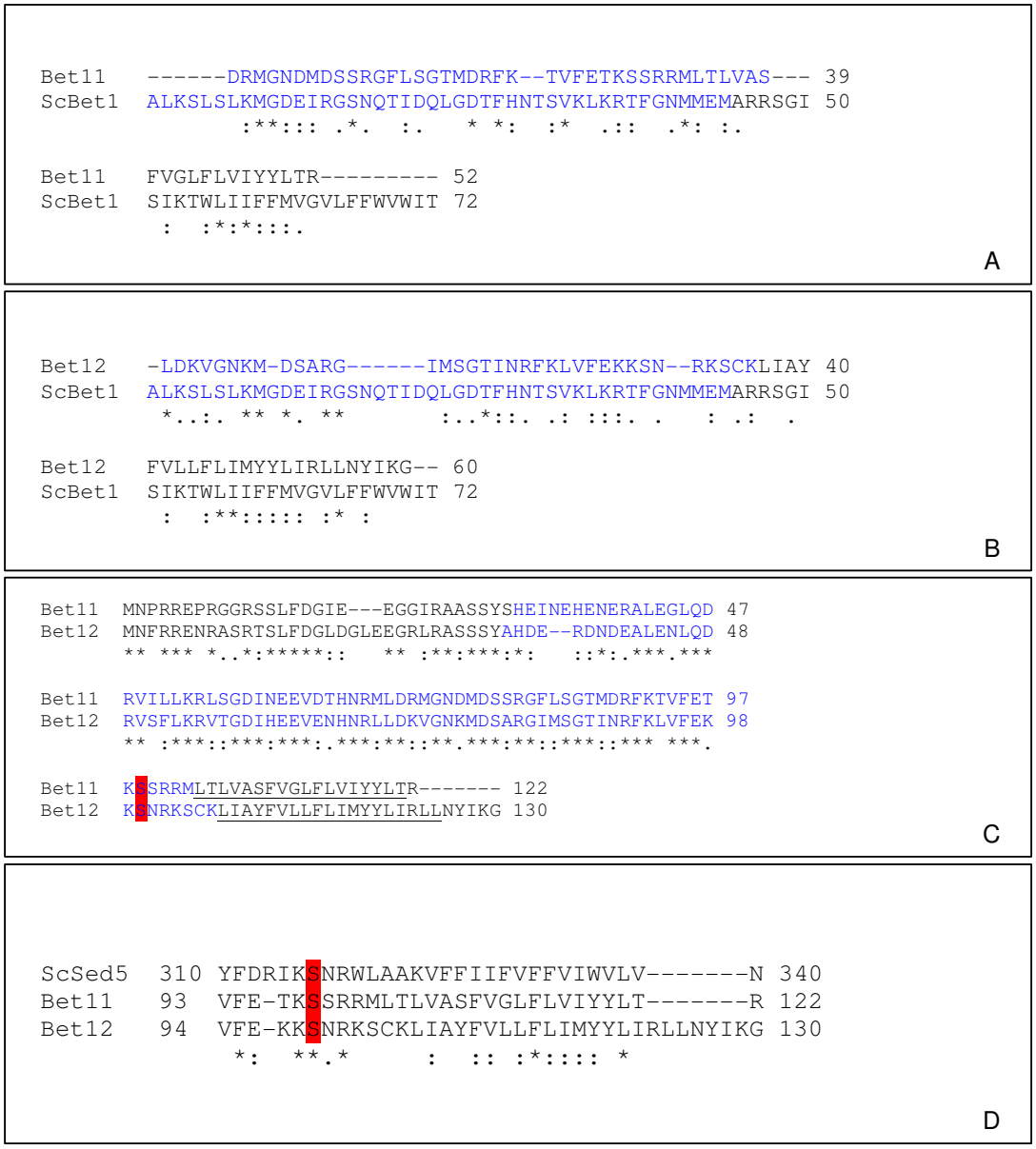
Bet11 ------DRMGNDMDSSRGFLSGTMDRFK--TVFETKSSRRMLTLVAS--- 39
ScBet1 ALKSLSLKMGDEIRGSNQTIDQLGDTFHNTSVKLKRTFGNMMEMARRSGI 50
Bet11 FVGLFLVIYYLTR---------- 52
ScBet1 SIKTWLIIFFMVGVLFFWVWIT 72
A
Bet12 -LDKVGNKM-DSARG------IMSGTINRFKLVFEKKSN--RKSCKLIAY 40
ScBet1 ALKSLSLKMGDEIRGSNQTIDQLGDTFHNTSVKLKRTFGNMMEMARRSGI 50
Bet12 FVLLFLIMYYLIRLLNYIKG-- 60
ScBet1 SIKTWLIIFFMVGVLFFWVWIT 72
B
Bet11 MNPRREPRGGRSSLFDGIE---EGGIRAASSYSHEINEHENERALEGLQD 47
Bet12 MNFRRENRASRTSLFDGLDGLEEGRLRASSSYAHDE--RDNDEALENLQD 48
Bet11 RVILLKRLSGDINEEVDTHNRMLDRMGNDMDSSRGFLSGTMDRFKTVFET 97
Bet12 RVSFLKRVTGDIHEEVENHNRLLDKVGNKMDSARGIMSGTINRFKLVFEK 98
Bet11 KESSRRMLTLVASFVGLFLVIYYLTR------- 122
Bet12 KENRKSCKLIAYFVLLFLIMYYLIRLLNYIKG 130
C
ScSed5 310 YFDRIKSNRWLAAKVFFIIFVFFVIWVLV-------N 340
Bet11 93 VFE-TKSSRRMLTLVASFVGLFLVIYYLT-------R 122
Bet12 94 VFE-KKSNRKSCKLIAYFVLLFLIMYYLIRLLNYIKG 130
D

1.4 Studying the secretory pathway *in vivo*

Traditionally, the secretory pathway has been studied using a combination of three different approaches: microscopy, biochemistry and genetics. In the last ten years after the identification and cloning of the gene encoding green fluorescent protein (GFP) and the development and availability of confocal microscopes, live cell imaging has became a major experimental approach to study the secretory pathway.

GFP is a 27 kDa protein that emits green fluorescence if excited by UV or blue light (Shimomura et al., 1962; Chalfie et al., 1994). GFP can be fused with specific secretory proteins to follow movement through the endomembrane system (Brandizzi et al., 2004). This method permits the use of several known proteins fused with GFP as markers of specific endomembrane compartments. This is the case, for instance, of ER-Retention Defective Receptor 2 (ERD2) and sialyltransferase (ST) (see Table 1.1) which were the first two fluorescent markers used to visualize the Golgi stacks in plant cells (Boevink et al., 1998). ERD2 is also used to visualize the ER (Boevink et al., 1998). In addition, there are several spectral variants of GFP that allow simultaneous visualization of multiple compartments in the same cell (Brandizzi et al., 2004).

For the study of the secretory pathway, confocal microscopy is a convenient tool as it captures light emitted from one single plane of a sample. This improves imaging by increasing the signal to noise ratio. This is achieved by a pinhole, which blocks the light coming from other planes besides the one in focus. In this manner, only the light coming from the in-focus plane can reach the detector. The light emitted from the sample is collected by a photomultiplier that transmits the information to a computer that forms an image that represents an optical section of the sample (Paddock, 2000; Zeiss web site:

www.zeiss.com).

GFP technology and confocal microscopy offer the possibility of studying living cells by imaging, which is crucial to gaining an understanding of the mechanisms involved in the dynamic secretory pathway.

MARKER	LOCALIZATION	REFERENCES
Erd2	ER and Golgi	Boevink et al., 1998
ST	Golgi	Boevink et al., 1998
T-CASP	Golgi	Renna et al., 2005
Arf1	Golgi and Post-Golgi	Matheson et al., 2007; Stefano et al., 2006a
Ara6	Early Endosomes	Ueda et al., 2004
Ara7	Late Endosomes	Ueda et al., 2004

Table 1.1 Protein markers used in this study and their intracellular localization.

1.5 Objectives

1. Identification of amino acid sequence(s) or protein motif(s) important for Bet11 and Bet12 intracellular sorting.
2. Studying the role of phosphorylation in Bet11 and Bet12 trafficking and function.
3. Understanding the role of Bet11 and Bet12 in vesicular trafficking.

1.6 Significance

This analysis of Bet11 and Bet12 is significant for at least five reasons:

1. The identity of organelles is dictated by their protein content and protein composition on the cytosolic surface. Therefore understanding how proteins are targeted to one compartment can provide clues on how the identity of organelle is established.
2. Bet11 and Bet12 have a high degree of identity. My work shows that they are localized in different compartments. How they achieve this is unknown. Therefore understanding the targeting mechanism of these two proteins can provide insights on protein targeting mechanisms that may form the basis of organelle biogenesis.
3. Despite their importance in the secretion processes in plant cells, the roles of SNAREs is only now beginning to emerge. Therefore, by studying the cellular role of Bet11 and Bet12 we will gain further insights on the role of Qc SNAREs in plant cells.
4. In the *Arabidopsis thaliana* genome, there are 54 genes coding for SNAREs (18

Qa, 8 Qb, 11 Qc and 14 R and 3 SNAP-25). It is still unclear if every single SNARE has a particular function or if a genetic redundancy exists. Bet11 and Bet12 have high sequence identity (high sequence identity: 50-95%; medial sequence identity 25-49%; low sequence identity: >25%), but they have different intracellular localization. Functional characterization of Bet11 and Bet12 may provide proof of the presence or absence of redundancy between SNAREs.

5. The SNARE motifs of Bet11 and Bet12 have medial sequence identity with yeast Bet1 and rBet1, but the intracellular localizations of these proteins are different. It is possible that all these proteins derive from a unique protein but during evolution they have developed different functions. Understanding the functions of Bet11 and Bet12 may provide more information about the divergent evolution of yeast and plants.

2. MATERIALS AND METHODS

2.1 Materials

2.1.1 Biological materials

To amplify all plasmids used in this study, the *Escherichia coli* strain MC1061 (Invitrogen) was used. *Nicotiana tabacum* cv Petit Havana was used for transient expression and confocal experiments. The plants were grown in a growth chamber in Sungro Horticulture Mix-1 (Canada soil). The growth conditions were set at 25°C with 16 h light and 8 h dark. The light irradiance was 200 $mE.\mu^{-2}.sec^{-1}$. The *Agrobacterium tumefaciens* strain used for the tobacco leaf infiltration was GV3101. The cDNA of *BET11* (109J2 clone) was purchased from ABRC (www.arabidopsis.org). *Arabidopsis thaliana* cv Columbia were grown in Pro-Mix "BX" soil (Premier Horticulture).

2.1.2 Growth media

The formulations of the growth media used in this study are listed in Table A1 of the Appendix. Luria Bertani medium (LB) was used to grow *E. coli* (MC1061 strain) and *A. tumefaciens* (GV3101 strain). YT medium was used to grow *E. coli* in preparation for the transformation of competent cells.

2.1.3 Solutions, enzymes, chemicals and primers

Solutions, enzymes, kits and primers used in this study are listed in Table A2, A3, A4 of the Appendix. Chemicals and enzymes were purchased from Fermentas (www.fermentas.com), Invitrogen (www.invitrogen.com), NEB (www.neb.com), Promega (www.promega.com), Qiagen (www.qiagen.com), Sigma Aldrich (www.sigma-aldrich.com) and VWR International (www.vwr.com).

2.2 Methods

2.2.1 Molecular cloning

Standard molecular techniques used in this study are described in Sambrook *et al*. (1989). mGFP5 (Haseloff *et al*., 1997) and EYFP (Clontech Inc., California, USA) were used to obtain the fluorescent tagged proteins used in this research. The binary vector pVKH18En6 was already present in Dr. Brandizzi's laboratory and was used to clone DNA and to express the fluorescent tagged proteins in tobacco leaves (Figure 2.1) (Batoko *et al*., 2000). Mutant sequences were generated by site direct mutagenesis using specific primers and clones were sequenced (PBI/NRC, Saskatoon; RTSF/MSU, East Lansing) to check mutations while chimaeric sequences were generated by overlapping polymerase chain reaction (PCR) using specific primers. A standard protocol for PCR was modified depending on the specific primer sequence (Table A5 and A6 of the Appendix). The QIAquick PCR Purification Kit (Qiagen) was used for the purification of PCR products. The QIAquick Gel Extraction Kit (Qiagen) was used for DNA purification from agarose gel.

I have generated fluorescent fusions of Bet11 and Bet12 using YFP (Bet11-YFP and

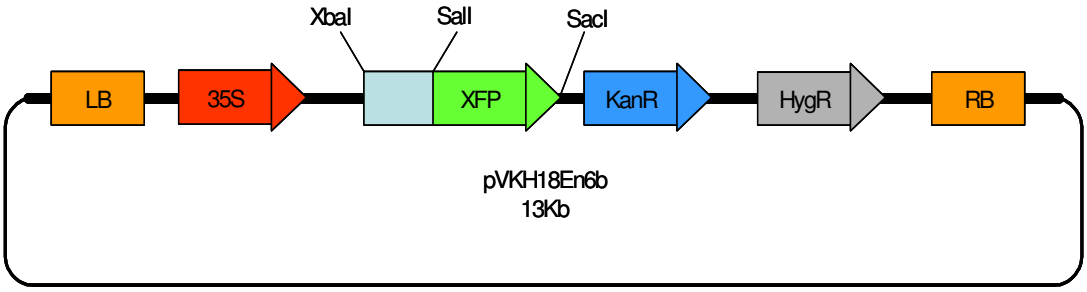

Figure 2.1 Schematic representation of the binary vector pVKH18En6b. The plasmid carries the left (LB) and right (RB) border flanking the T-DNA region, the gene for kanamycin resistance (KanR) and for hygromycin resistance (HygR) for selection in bacteria and in plants respectively. Upstream to the gene of a fluorescent protein (XFP, that can be GFP, YFP or CFP), the vector carries an *Xba*I and *Sal*I used to clone the sequences of interest under the 35S promoter from the cauliflower mosaic virus (Batoko et al., 2000).

Bet12-YFP) in order to study their intracellular distribution. This was achieved by using a co-expression analysis of the construct with specific fluorescent markers for the secretory pathway. The coding sequence of Bet11 was amplified directly from the ABRC clone 109J2. The Bet12 coding sequence was amplified from *Arabidopsis* cDNA obtained from total mRNA reverse-transcription (RT-PCR). After amplification, the two coding sequences were inserted upstream to YFP, using the unique *Xba*I and *Sal*I restriction sites in the pVKH18-En6 binary vector (Figure 2.1).

2.2.2 Agarose gel electrophoresis

Agarose gel electrophoresis was used to analyze DNA and RNA preparations. The standard agarose concentration used was 1% in 1X TAE buffer. To visualize nucleic acids under UV light, ethidium bromide was added to the gel at a final concentration of 0.5 μg/ml. The voltage applied to run the electrophoresis was 100 V. The nucleic acid samples were prepared adding 1/5 volume of 5x loading buffer (Table A2 of the Appendix).

2.2.3 Preparation of *E. coli* MC1061 competent cells

E. coli MC1061 cells were streaked on LB plates containing 50 μg/ml streptomycin and allowed to grow overnight at 37 °C. A single colony was used to inoculate 3 ml 2X YT medium, incubated at 37 °C with 200 rpm shaking. This pre-inoculation was allowed to grow to $O.D._{600} = 0.3$ then it was used to inoculate 200 ml of pre-warmed (37 °C) 2X YT medium and incubated at 37 °C with 200 rpm shaking. At $O.D._{600} = 0.480$, the culture was divided in four sterile 50 ml conical tubes and left on ice for 5 min. Then the culture was pelleted at 3000 *g* for 20 min in a pre-cooled swing-out rotor (4 °C)

(Beckman Coulter, Allegra X-22 centrifuge) and the supernatant was discarded. The pellet was resuspended in 80 ml ice-cold TFP I and left on ice for 5 min. The cells were pelleted as previously described and then resuspended in 8 ml of TFB II and placed on ice for 15 min. The cells were aliquoted into pre-chilled Eppendorf tubes, frozen in liquid nitrogen and stored at -80°C.

2.2.4 Preparation of *A. tumefaciens* GV3101 competent cells

A. tumefaciens GV3101 cells were streaked on an LB plate containing 15 µg/ml of gentamycin and allowed to grow at 28 °C for 48 h. A single colony was inoculated in liquid LB medium with antibiotic and the pre-culture was grown overnight at 28 °C with 250 rpm shaking. Two ml of this pre-culture were used to inoculate 50 ml of LB liquid medium with gentamycin and grown under the same conditions until an OD_{600} between 0.5 and 1 was reached. The culture was transferred to a 50 ml conical tube and left on ice for 10 min. Finally, the cells were pelleted for 10 min at 5000 rpm at 4 °C in a pre-cooled swing-out rotor (Beckman Coulter, Allegra X-22 centrifuge) and the pellet was resuspended in 1 ml of sterile cold 20 mM $CaCl_2$. Cells were aliquoted in pre-chilled Eppendorf tubes, frozen in liquid nitrogen and stored at -80°C.

2.2.5 Competent *E.coli* transformation

A heat shock procedure was used to transform *E. coli* competent cells. Ten ng of DNA were added to 100 µl of cells and the tube was left on ice for 20 min. The tube was then transferred to an incubation temperature of 42 °C for 30 seconds and quickly transferred to ice for 5 min. Seven hundred µl of LB medium were added to the cells and the culture was incubated for 1 hr at 37 °C with 170 rpm shaking. The cells were then

plated on an LB agar plate with selective antibiotics and grown overnight at 37 °C.

2.2.6 Competent A. tumefaciens transformation

A heat shock procedure was used to transform *A. tumefaciens*. Fifteen to 20 ng of DNA were added to 50 µl of cells and the tube was left on ice for 5 min, transferred to liquid nitrogen for 5 min and incubated at 37 °C for 5 min. Seven hundred µl of LB were added to the cells and the culture was incubated for 6 hr at 28 °C with shaking at 130 rpm. Cells were then plated on an LB agar plate containing the appropriate selective antibiotics and grown for two days at 28 °C.

2.2.7 Extraction of plasmid DNA from *E. coli* clones (Minipreps)

A single *E. coli* colony from a plate was use to inoculate 3 ml of LB medium plus antibiotic and grown overnight with shaking at 180 rpm. Cells were pelleted at 13000 rpm and resuspended in 250 µl P1 (see Table A2 in Appendix) solution supplemented with 2 µl/ml of RNAase A (Fermentas). After 15 min at room temperature, 250 µl P2 (see Table A2 in Appendix) solution were added, gently mixed and incubated for 5 min at room temperature. Three hundred and fifty µl of ice-cold P3 (see Table A2 in Appendix) solution were added, gently mixed and left on ice for 10 min. This was followed by centrifugation for 10 min at 14000 rpm (Beckman Coulter, Microfuge 22R Refrigerated Microcentrifuge) and the supernatant was transferred to a new Eppendorf tube. Seven hundred and fifty µl of isopropanol were added to the previously transferred supernatant and the solution was vortexed. DNA was pelleted at 14000 rpm for 30 min (Beckman Coulter, Microfuge 22R Refrigerated Microcentrifuge). The supernatant was discarded and the pellet was left to dry at room temperature. To resuspend DNA, 50 µl

of sterile distilled water were added.

2.2.8 Transient expression system in tobacco epidermal leaves

Four week old tobacco plants grown in a greenhouse at 25 °C were infected with *A. tumefaciens*. For the agroinfiltration procedure, *A. tumefaciens* were grown to stationary phase in 3 ml LB medium at 28 °C for 16 hours with shaking at 180 rpm. One and a half ml of cells were centrifuged for 5 min at 8000 rpm (Beckman Coulter, Microfuge 22R Refrigerated Microcentrifuge) and resuspended in 1 ml of infiltration (IF) buffer (see Table A2 in Appendix). Cells were centrifuged and resuspended in IF twice to eliminate any antibiotic residue. The OD_{600} of the cell suspension was determined and the cells were diluted with IF to obtain the optimal OD that varies between constructs (from 0.05 to 0.2). Bacterial cells were infiltrated into the abaxial air space of tobacco leaves using a sterile 1 ml syringe without a needle (Kapila *et al*. 1997, Batoko *et al*., 2000).

2.2.9 Sampling and imaging

Seventy-two h after *A. tumefaciens* infection of the lower epidermis, transformed leaves were analyzed using an upright or inverted laser confocal microscope (Zeiss 510 META, 63x water or oil immersion objective).

For imaging expression of yellow fluorescent protein (YFP) constructs, a 514 nm excitation line of an argon ion laser was used. For imaging coexpression of YFP and GFP constructs and for GFP constructs alone, excitation lines of an argon ion laser of 514 nm for YFP and 458 nm for GFP were used. To detect cyan fluorescent protein (CFP) constructs a violet diode laser (405 nm) was used. The laser intensity was between 2 and 5 % for YFP, 10-25 % for GFP and 15-25 % for CFP. Appropriate

controls were carried out to exclude the possibility of energy transfer between fluorochromes and cross-talk. The pinhole diameter range was between 1 and 3 μm. Zoom was used to acquire images and a level 4 zoom was used to observe the cells in detail. The detector gain was set between 700 and 800. The line averaging used was 16. LSM 5 Image Browser (Zeiss) was used to process the images. The images were assembled using Microsoft Power Point.

2.2.10 Extraction of genomic DNA from *Arabidopsis* leaves

A small piece of leaf, 0.25 cm^2, was homogenized in an Eppendorf tube using a pestle. One hundred μl of Extraction Buffer (see Table A2 in Appendix) were added in the tube and the tissue was further disrupted. After adding 100 μl of Extraction Buffer, the sample was vortexed for a few seconds and then centrifuged for 2 min at 13000 rpm (Beckman Coulter, Microfuge 22R Refrigerated Microcentrifuge). One hundred and seventy μl of the supernatant were transferred into a new tube and 170 μl of isopropanol were added. The sample was left at room temperature for 5 min and then centrifuged for 5 min at 13000 rpm. The supernatant was discarded and the DNA was left to dry. The dry DNA was subsequently resuspended in 50 μl of sterile water.

2.2.11 RNA extraction and RT-PCR

The extraction of RNA from *Arabidopsis* leaves was done using the RNeasy Plant Mini Kit (Qiagen). Reverse transcription, to produce cDNA, was done using the SuperScript III First-Strand Synthesis SuperMix (Invitrogen) following the protocol described in Table A9 of the Appendix.

2.2.12 *In vitro* pollen germination

The basic medium for the *in vitro* pollen germination contains 5 mM MES (pH 5.8 adjusted with Tris), 1 mM KCl, 10 mM $CaCl_2$, 0.8 mM $MgSO_4$, 1,5 mM boric acid, 1% (w/v) agar, 16.6% (w/v) sucrose, 3.65% (w/v) sorbitol, 10 µg/ml myo-inositol (Fan et al., 2001). The medium was prepared with double distilled sterile water and heated to 100°C for 2 min. A few drops of liquid medium were put on a slide and allowed to solidify.

Anther-dehisced flowers were collected from several plants. The anthers were carefully dipped onto the surface of the germination medium to transfer the pollen grains.

The slides were transferred to a chamber at 25°C with 100% humidity. After a 4-6 h incubation period, the germination of pollen grains was observed under the microscope.

2.2.13 Pistil preparation and staining for *in vivo* pollen study

Pistils were collected from several flowers and fixed overnight in a solution of 70% ethanol-glacial acetic acid (3:1 v/v). Pistils were transferred in an 8 N KOH solution for 24 hours. After 5 washes in water, pistils were stained with a decolorized aniline blue solution (0.1% aniline blue in 0.1 M K_3PO_4). Pollen tube growth was analyzed under the confocal microscope.

2.2.14 NaCl treatment of *Arabidopsis* roots

Wild type and mutant *Arabidopsis* seeds were surface-sterilized with 30% bleach rinsed with sterile water and incubated at 4°C to break seed dormancy. After 2 days seeds were dispersed on a plate containing 4.4 g/l Murashige and Skoog basal medium

(Sigma-Aldrich) 2% sucrose and 0.8% tissue culture grade agar and transferred to a growth chamber (16 h light/ 8 h dark cycle at 24°C and light intensity of 30 $\mu Exm^{-2}\ s^{-1}$). After 10 day-old roots were dipped in a 250 mM NaCl solution for 10 min and stained in a 40 μM solution of FM4-64 and the vacuolar morphology was observed by confocal microscopy.

3. RESULTS

3.1 Intracellular localization of Bet11 and Bet12

Prior to understanding the role of Bet11 and Bet12 in plant cells, it is essential to establish their intracellular distribution. To my knowledge, there is no literature describing the intracellular localization of Bet12 and there is little information about the intracellular localization of Bet11.

Using the confocal microscope, I have demonstrated that Bet11-YFP and Bet12-YFP have different intracellular distributions in tobacco leaves (Figure 3.1). Bet12-YFP co-localized with the ER-Golgi stacks marker ERD2-GFP on the Golgi stacks. Bet11-YFP co-localized with ERD2-GFP on the ER and Golgi stacks in addition to non-Golgi punctate structures. The nature of these structures was unknown; however, we hypothesized that they were post-Golgi compartments. In fact, in *Arabidopsis* protoplasts Uemura et al. (2004) showed that Bet11 labeled the *trans*-Golgi and this localization might suggest a role for this protein in post-Golgi traffic.

To prove the presence of Bet11-YFP on post-Golgi compartments, I co-expressed Bet11-YFP with Arf1-GFP (Figure 3.2). Arf1 is a small GTPase involved in retrograde transport from the Golgi stacks to the ER (Antonny et al., 2005; Matheson et al., 2007). It labels the Golgi stacks but is also present on additional punctate structures that detach from the Golgi stacks and that have been identified as part of the endocytic route (Matheson et al., 2007; Stefano et al., 2006a) (see Table 1.1). Bet11-YFP and

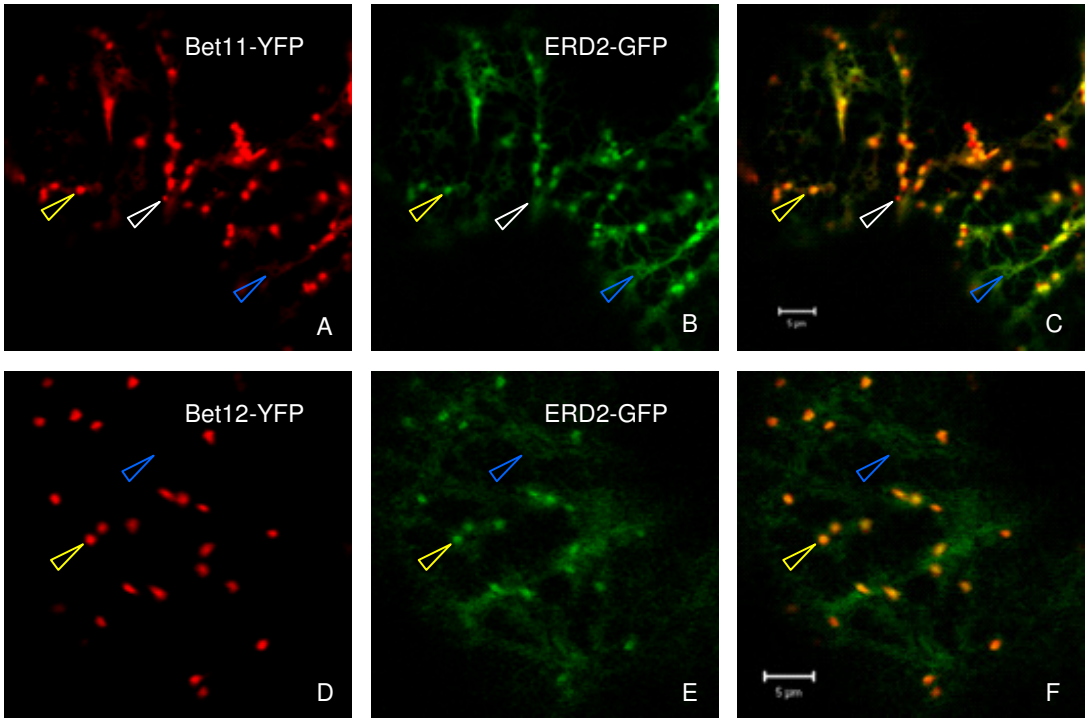

Figure 3.1 Intracellular distribution of Bet11-YFP and Bet12-YFP. Confocal images of tobacco leaf epidermal cells 3 days after *A. tumefaciens* infiltration with Bet11-YFP, Bet12-YFP ($O.D._{600}$= 0.05) and ERD2-GFP ($O.D._{600}$= 0.2). Bet11-YFP **(A)** co-localized with ERD2-GFP **(B)** on the ER (blue arrowhead) and on the Golgi stacks (yellow arrowheads, panel A, B and C). Bet11-YFP also labeled non-Golgi punctate structures (white arrowheads panel A, B and C). Bet12-YFP **(D)** co-localized with ERD2-GFP **(E)** only on the Golgi stacks (yellow arrowheads, panel D, E and F). **(C)** Merged image of A and B. **(F)** Merged image of D and E. Scale bars: 5 µm.

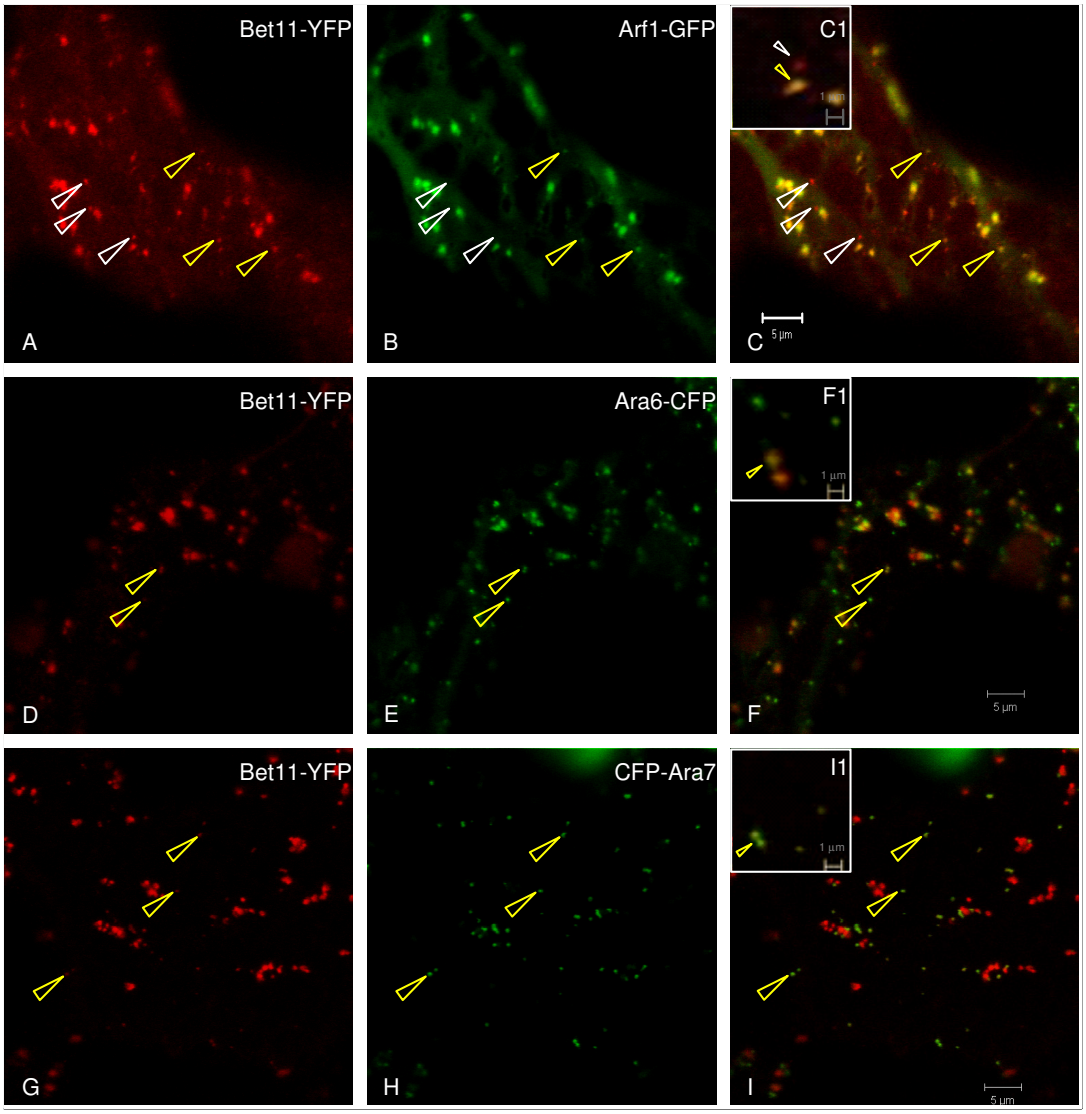

Figure 3.2 Bet11-YFP labels endosomes. Confocal images of tobacco leaf epidermal cells 3 days after *A. tumefaciens* infiltration with Bet11-YFP, Arf1-GFP, Ara6-CFP and CFP-Ara7 ($O.D._{600}$ = 0.05). Panel **A**, **B** and their merged image **C** show that Bet11-YFP co-localized with Arf1-GFP on the Golgi stacks and on the endocytic compartments (yellow arrows) but Bet11 was also detectable on distinct punctate structures (white arrows). **C1**, high magnification image of Bet11-YFP co-expressed with Arf1-GFP. The co-expression of Bet11-YFP (**D** and **E**) with the late endosome marker Ara6-CFP **(E)** and the early endosomes marker CFP-Ara7 **(H)** showed that the non-Golgi punctate structures labeled by Bet11 were early and late endosomes (yellow arrowheads). **(F)** Merged image of D and E. **(I)** Merged image of G and H. F1 high magnification image of Bet11-YFP co-expressed with Ara6-CFP. **I1**, high magnification image of Bet11-YFP co-expressed with CFP-Ara7. Scale bars 5 µm.

Arf1-GFP co-localized on the Golgi stacks and on Arf1 endocytic compartments.

Nevertheless, Bet11 is also present on distinct compartments. This clearly indicated that the punctate structures of Bet11 are a heterogeneous population of different compartments. To obtain additional evidence for the localization of Bet11 on post-Golgi compartments, I co-expressed Bet11-YFP with Ara6-CFP and CFP-Ara7. Ara6 and Ara7 are Rab GTPases, a group of proteins involved in vesicular transport, that label two populations of endosomes that partially overlap (Ueda et al., 2004) (see Table 1.1). The co-expression of Bet11-YFP with these two Rab proteins showed that Bet11 labeled large organelles (Golgi stacks) and small organelles and these smaller compartments co-localized with Ara6 and Ara7 (Figure 3.2). These results confirmed the presence of Bet11 in endocytic compartments and suggested a role for this SNARE in post-Golgi traffic.

Despite the sequence identity between Bet11 and yeast Bet1 and the possibility of Bet11 complementing the *sft-1* mutation (SFT-1 is a member of Bet1 family in yeast) (Tai et al, 2001), it is evident that *Arabidopsis* Bet11 has a different role in protein sorting that involves not only the ER-Golgi stacks transport system but also post-Golgi traffic.

3.2 Identification of the region important for Bet11 and Bet12 targeting

As previously demonstrated, Bet11 and Bet12 have a different intracellular distribution (Figure 3.1). In the literature very little is known about target signals of SNARE proteins. I was interested in determining the protein region that contains the sorting signal(s) of Bet11 and Bet12. To achieve this objective I generated different truncated and chimaeric proteins of these two SNAREs fused with YFP. In some cases I used the transmembrane domain of a type II transmembrane protein involved in

vesicular transport between the ER and Golgi stacks, the *Arabidopsis* Sec12 (Bar-Peled & Raikhel, 1997). The constructs and the results are summarized in Figure 3.3.

The co-expression of the transmembrane domain of Bet11 fused with YFP (mBet11) and the Golgi stacks marker T-CASP-GFP (see Table 1.1) in tobacco leaf epidermal cells showed that this domain of Bet11 was not localized on the Golgi stacks but it labeled only the ER tubules (Figure 3.4). This result suggested that the transmembrane domain of Bet11 does not contain signals for ER export. On the contrary, the transmembrane domain of Bet12 fused to YFP (mBet12) was distributed not only on the ER but also on the Golgi stacks (Figure 3.4), suggesting that the transmembrane domain alone is able to transport Bet12 to its final compartment.

The absence of ER export signals in the transmembrane domain of Bet11 prompted me to focus the search for the sorting domain on the cytoplasmic region of this protein. To prove the relevance of this region in Bet11 targeting I have fused the cytoplasmic domain of Bet11 with the transmembrane domain of Bet12 (Bet11-12-YFP) and *vice versa* (Bet12-11-YFP). The chimaeric protein Bet11-12 had the same intracellular distribution of Bet11 (Figure 3.5). These results proved that the CT region of Bet11 contains the signal for proper targeting of this protein to the Golgi stacks and non-Golgi punctate structures. At the same time, the chimaeric protein Bet12-11 is only localized on the Golgi stacks as is Bet12 (Figure 3.5). It is possible that the cytoplasmic region of Bet12 contains an additional signal for transport to the Golgi stacks that acts in synergy with the transmembrane domain signal for the proper localization of Bet12.

Further evidence to support the relevance of the cytoplasmic domain of Bet11 and Bet12 in protein targeting came from studying the intracellular distribution of two other chimaeric proteins: Bet11-Sec12-YFP and Bet12-Sec12-YFP. These proteins have been

obtained by fusing the transmembrane domain of Sec12 with the cytosolic domains of Bet11 and Bet12 respectively. Figure 3.6 shows that the chimaeric proteins Bet11-Sec12-YFP and Bet12-Sec12-YFP had the same intracellular distribution as Bet11-YFP and Bet12-YFP respectively. These data confirm that the signals for ER export likely reside in the cytosolic portion of the two SNAREs and, in the full length SNARE, these signals are more important than transmembrane domains to facilitate the membrane associate traffic.

To determine whether the cytoplasmic region of Bet11 and Bet12 fused with YFP (cBet11 and cBet12) was able to bind membranes in the absence of the transmembrane domain, I expressed the fusions in tobacco leaf epidermal cells. Confocal analyses showed that cBet11 localized in the cytosol (Figure 3.6), showing that this region of the protein cannot overcome the necessity of a transmembrane domain for proper trafficking of this SNARE. Bet12 fusion was also localized in the cytosol but it was partially detected on the Golgi stacks too. This result suggested that the cytosolic domain of Bet12 may interact with SNAREs on the Golgi stacks determining the localization of this domain. It can not be excluded that the interaction between full length Bet12 and other SNAREs happens naturally during Bet12 traffic and this interaction can be essential for Bet12 sorting.

To isolate the cytosolic region carrying the targeting signal(s) of Bet11 and Bet12, I have substituted the first 58 amino acids at the N-terminal region of Bet12-11 with the first 57 amino acids of the N-terminal region of Bet11; the chimaeric protein obtained was called Bet11-12-11-YFP. A chimaeric protein, Bet12-11-12-YFP, was obtained by substituting the first 57 amino acids at the N-terminal region of Bet11 with the first 58 amino acids at the N-terminal region of Bet12. Bet12-11-12-YFP localized to the Golgi

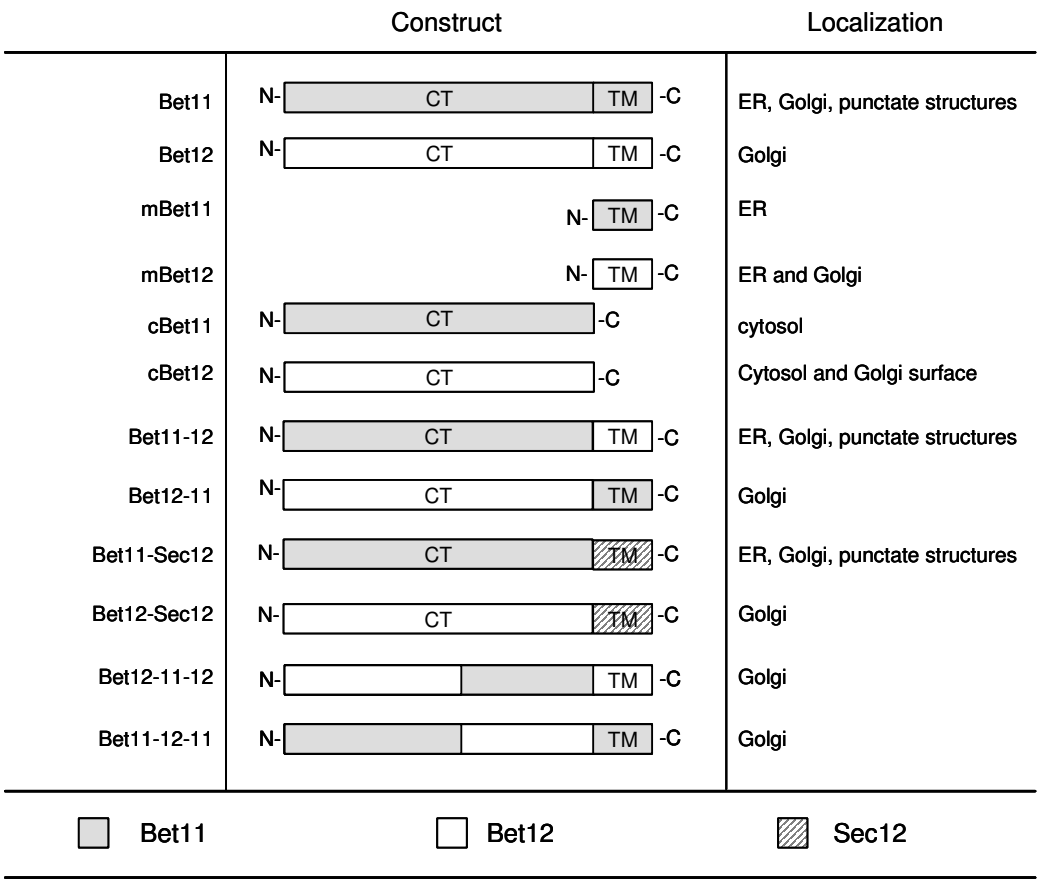

Figure 3.3 Schematic representation of the constructs used in this study and their intracellular localization. TM= transmembrane domain; CT= cytosolic domain; "m" = membrane; "c" = cytosolic. The fluorescent protein is fused at the C-terminus of each construct.

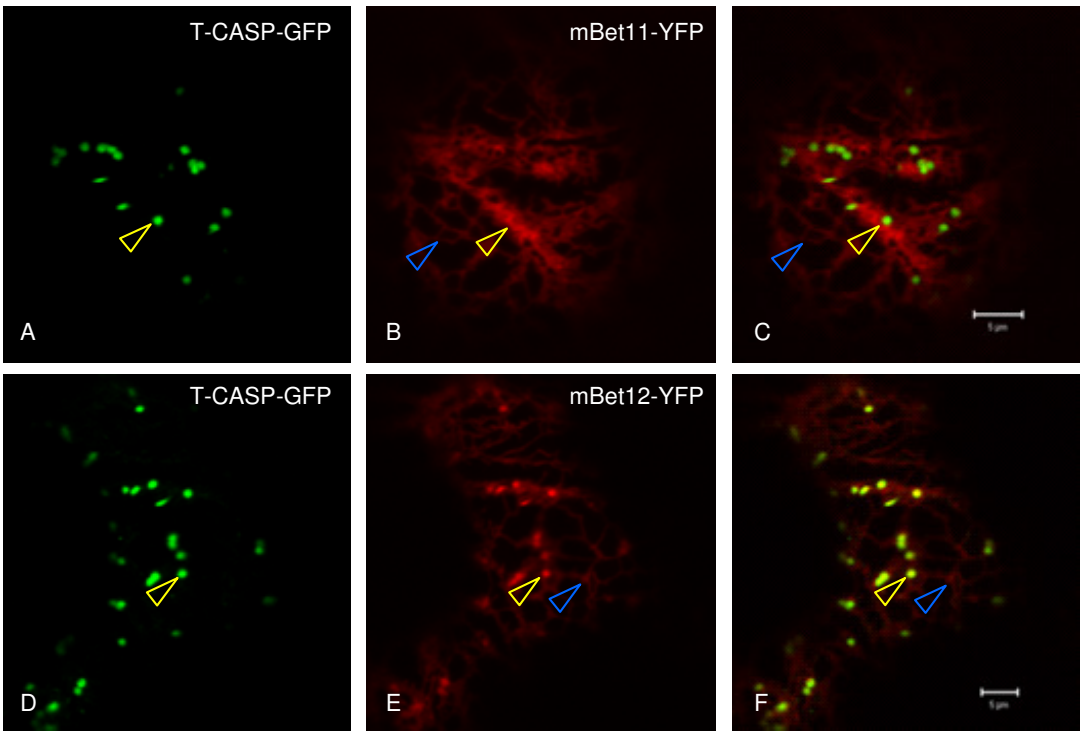

Figure 3.4 Intracellular distribution of mBet11 and mBet12. Confocal images of tobacco leaf epidermal cells 3 days after *A. tumefaciens* infiltration with mBet11-YFP, mBet12-YFP, the Golgi stacks marker T-CASP-GFP (Renna et al., 2005) ($O.D._{600}$= 0.05). mBet11-YFP (B) labeled the ER and never co-localized with T-CASP-GFP (A) on the Golgi stacks. (C) Merged image of A and B. On the contrary, mBet12 (E) labeled the ER but it also co-localized with T-CASP-GFP (D) on the Golgi stacks. (F) Merged image of D and E. Scale bars 5 µm.

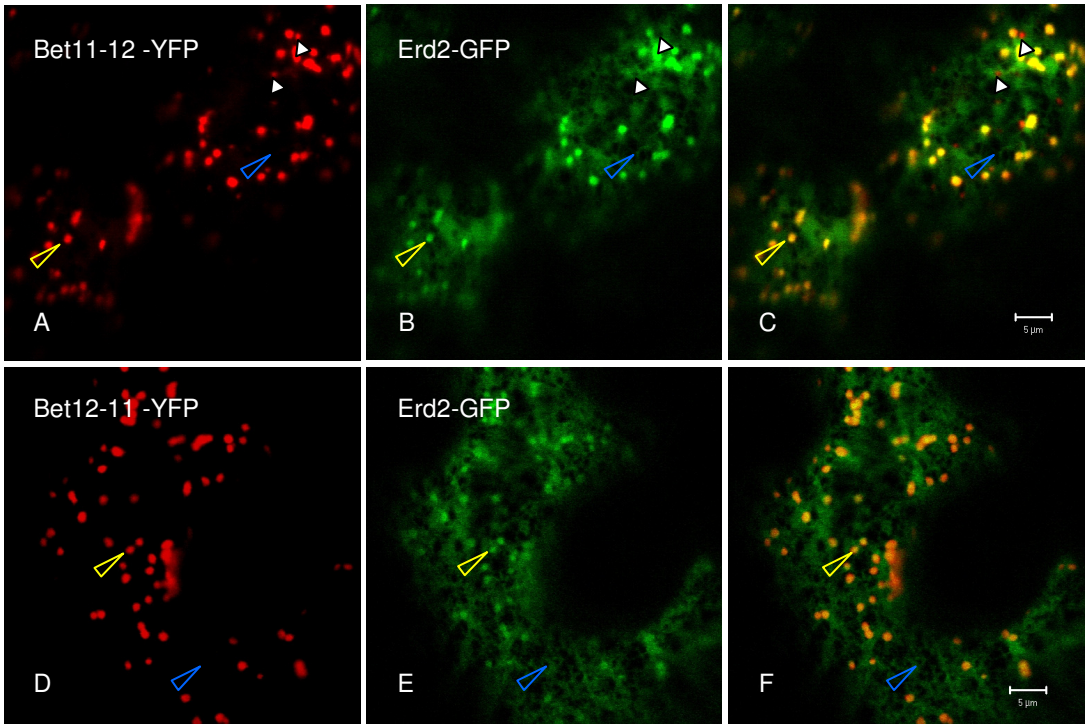

Figure 3.5 Intracellular distribution of Bet11-12-YFP and Bet12-11-YFP. Confocal images of tobacco leaf epidermal cells 3 days after *A. tumefaciens* infiltration with Bet11-12-YFP, Bet12-11-YFP ($O.D._{600}$ = 0.05) and ERD2-GFP ($O.D._{600}$ = 0.2). The construct Bet11-12-YFP (A) had the same intracellular distribution of Bet11-YFP. In fact Bet11-12-YFP co-localized with the ER-Golgi stacks marker ERD2-GFP (B) on the ER (blue arrowheads) and on the Golgi stacks (yellow arrowheads) and it also labeled the non-Golgi punctate structures (white arrowheads). (C) Merged image of A and B. Bet12-11-YFP (D), similar to Bet12-YFP, co-localized with ERD2-GFP (E) only on the Golgi stacks. (F) Merged image of D and E. Scale bars 5 µm.

Figure 3.6 The cytosolic regions of Bet11 and Bet12 contain a sorting signal for their intracellular targeting. Confocal images of tobacco leaf epidermal cells 3 days after *A. tumefaciens* infiltration with Bet11-Sec12-YFP, Bet12-Sec12-YFP, cBet11-YFP, cBet12-YFP, T-CASP-GFP ($O.D._{600}$ = 0.05) and ERD2-GFP ($O.D._{600}$ = 0.2). The construct Bet11-Sec12-YFP (A) had the same intracellular distribution of Bet11-YFP. In fact it co-localized with the ER-Golgi stacks marker ERD2-GFP (B) on the ER and on the Golgi stacks and it also labeled the non-Golgi punctate structures (white arrowheads). (C) Merged image of A and B. Bet12-Sec12-YFP (D), such as Bet12-YFP, co-localized with ERD2-GFP (E) only on the Golgi stacks (yellow arrowheads). (F) Merged image of D and E. The cytosolic Bet11 (H) was completely diffuse in the cytosol. cBet12 (K) was diffuse in the cytosol but it also labeled the Golgi stacks. (I) Merged image of G (T-CASP-GFP) and H. (L) merged image of J (T-CASP-GFP) and K. Scale bars 5 μm.

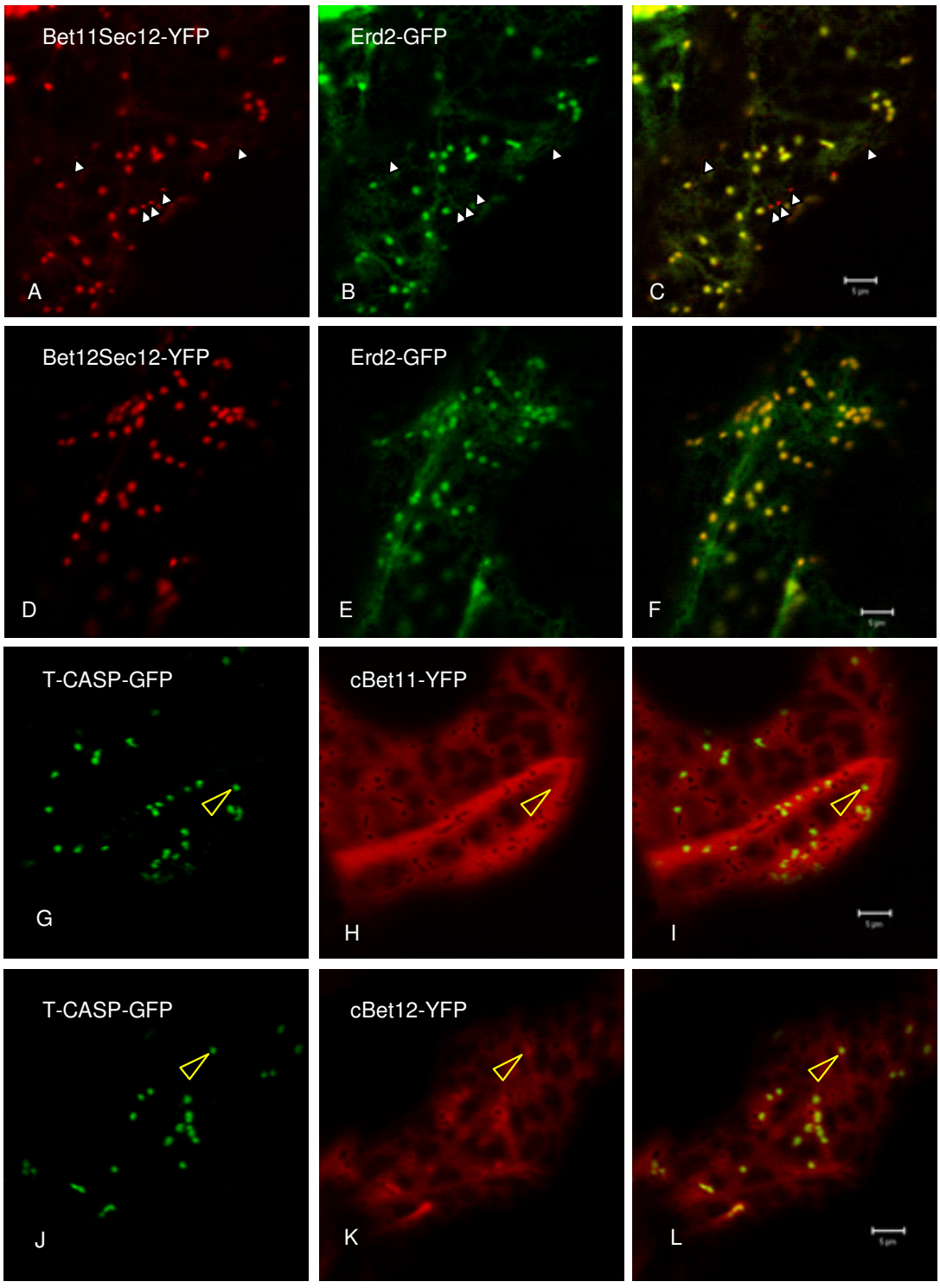
Bet11Sec12-YFP
Erd2-GFP
A
B
C
Bet12Sec12-YFP
Erd2-GFP
D
E
F
T-CASP-GFP
cBet11-YFP
G
H
I
T-CASP-GFP
cBet12-YFP
J
K
L

Figure 3.7 The distribution of Bet11 and Bet12 to the targeting compartments is the consequence of a combined influence of multiple domains. Panel A) Schematic representation of Bet11-12-11 and Bet12-11-12. **Panel B)** Confocal images of tobacco leaf epidermal cells 3 days after *A. tumefaciens* infiltration with Bet11-12-11-YFP, Bet12-11-12-YFP, T-CASP-GFP and ST-GFP ($O.D._{600}$ = 0.05). Bet11-12-11 YFP (A and G) labeled a heterogeneous population of compartments consisting in smaller (white arrowheads) and larger compartments (yellow arrowheads) but it always co-localized with the Golgi stacks markers T-CASP (B) and ST-GFP (H).The co-localization Bet12-11-12-YFP (D and J) with T-CASP-GFP (E) and ST-GFP (K) on the Golgi stacks was complete. (C) Merged image of A and B. (F) Merged image of D and E. (I) Merged image of G and H. (J) Merged image of K and L. Scale bars 5 μm.

Panel A)

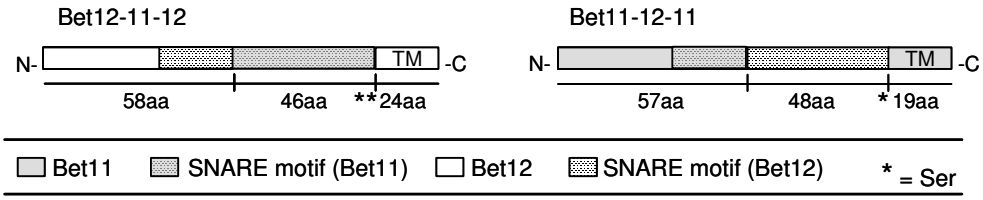

Panel B)

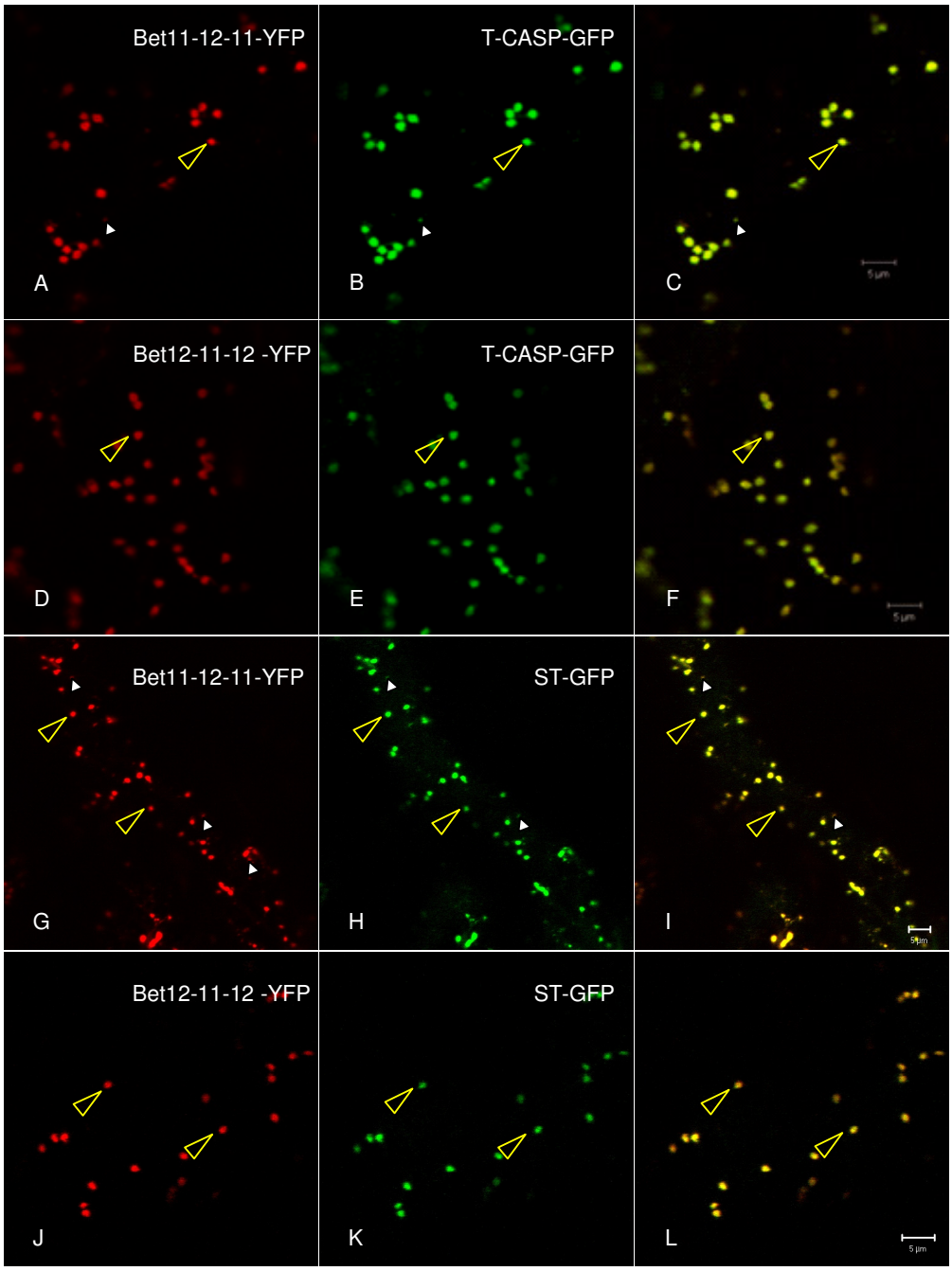

stacks (Figure 3.7). These results show that the central region of Bet11 does not contain a dominant signal for the transport of the chimaeric protein Bet12-11-12-YFP to the endocytic compartments.

The intracellular distributions of Bet11-12-11-YFP and Bet11-YFP were similar. In fact, Bet11-12-11-YFP labeled a heterogeneous population of organelles consisting of smaller and larger compartments (Figure 3.7). as does Bet11-YFP (Figure 3.1). Nevertheless, both these population of compartments co-localized with the Golgi stacks markers T-CASP-GFP and ST-GFP (Figure 3.7). It was evident that the chimaeric protein Bet11-12-11-YFP caused the mistargeting of Golgi stacks proteins to post-Golgi compartments. Possibly, the integrity of the SNARE motif is crucial for optimal functionality of Bet11 and to maintain the specificity of the post-Golgi traffic depending on Bet11. It is also possible that the central region of Bet11 is indirectly involved in cargo selection and the absence of this region causes post-Golgi traffic defects included mistargeting of Golgi stacks proteins to post-Golgi compartments.

I can conclude that the N-terminal region of Bet11 is sufficient to drive the exit of Bet11-12-11-YFP from the Golgi stacks. In this region I have identified a putative motif that might be crucial for the targeting of this SNARE (47-DxxxLL-52). In mammals, it was proven that this motif is important for sorting to post-Golgi compartments because it is recognized by clathrin adaptor complexes that drive the entrance of cargo proteins into clathrin coated vesicles (Miller et al., 2007).

The DxxxLL motif is present in the Bet11 but not in the Bet12 sequence and this could explain the difference in localization of these two SNAREs. To prove the relevance of this motif for Bet11 sorting, I have substituted two leucines (Leu51 and Leu52) with two alanines. The intention was to eliminate the putative sorting signal and

study its importance in Bet11 trafficking. Unfortunately, I did not have time to analyze the mutant.

In conclusion, my data suggest three key points:

A) The distribution of Bet11 and Bet12 to the target organelles is the result of a combined influence of multiple domains;

B) The positioning of these domains is not identical between the two SNAREs. In other words, the distribution of these proteins does not depend on a transplantable motif; and

C) The N-terminal region of Bet11 is essential for the correct targeting of this SNARE to post-Golgi compartments.

3.3 Studying the role of phosphorylation in Bet11 and Bet12 targeting

The yeast t-SNARE Sed5 (Qa), which is involved in ER-Golgi stacks trafficking, is phosphorylated on serine proximal to the transmembrane domain (Ser-317) (Weinberger et al., 2005). This post-translational modification influences Golgi stacks morphology and Sed5 trafficking (Weinberger et al., 2005).

In Dr. Brandizzi's laboratory, by sequence alignments, a colleague of mine, Laurent Chatre, identified that Ser-317 of yeast Sed5 is conserved in Bet11 and Bet12 sequences (Ser99 and Ser100, respectively). Bioinformatics analysis using online software, such as NetPhos 2.0 (http://www.cbs.dtu.dk/services/NetPhos/) and ScanProsite (http://www.expasy.org/tools/scanprosite/), has identified these serines as putative phosphorylation sites (Figure 1.3). To verify the effective phosphorylation of Bet11 and Bet12 and to study the effect of this modification on the activity of these two proteins I have used PCR-based site direct mutagenesis to substitute these serines with alanines

(S99A and S100A), in order to mimic a constitutive dephosphorylated status, and with aspartic acids (S99D and S100D), to mimic a constitutive phosphorylated status. Alanine is a non-polar amino acid structurally similar to non-phosphorylated serine and aspartic acid is a negatively charged amino acid similar in structure and charge to phosphorylated serine. These mutants have been fused with YFP to study their traffic *in vivo* by confocal microscopy.

The Bet11 mutants S99A-YFP and S99D-YFP formed aggregates that were visible on the bottom of the cells. It was not possible to establish where these aggregates were localized but considering the intracellular distribution of Bet11 it is possible to suppose that they were localized in the lumen of the ER. Bet11 mutants could partially reach the Golgi stacks, but the fluorescence in this compartment was very low compared with wild type Bet11 (Figures 3.8 and 3.9). These results suggest that mutations of serine in position 99 affect Bet11 traffic and/or the correct folding of this SNARE.

On the contrary, the mutations of the serine 100 in Bet12 did not seem to have an effect on Bet12 distribution (Figure 3.10).

I tried to biochemically verify the phosphorylation of Bet11 and Bet12 by immunoblot using a phospho-serine specific antibody. Unfortunately, I was unable to purify and detect these proteins and therefore unable to prove the phosphorylation.

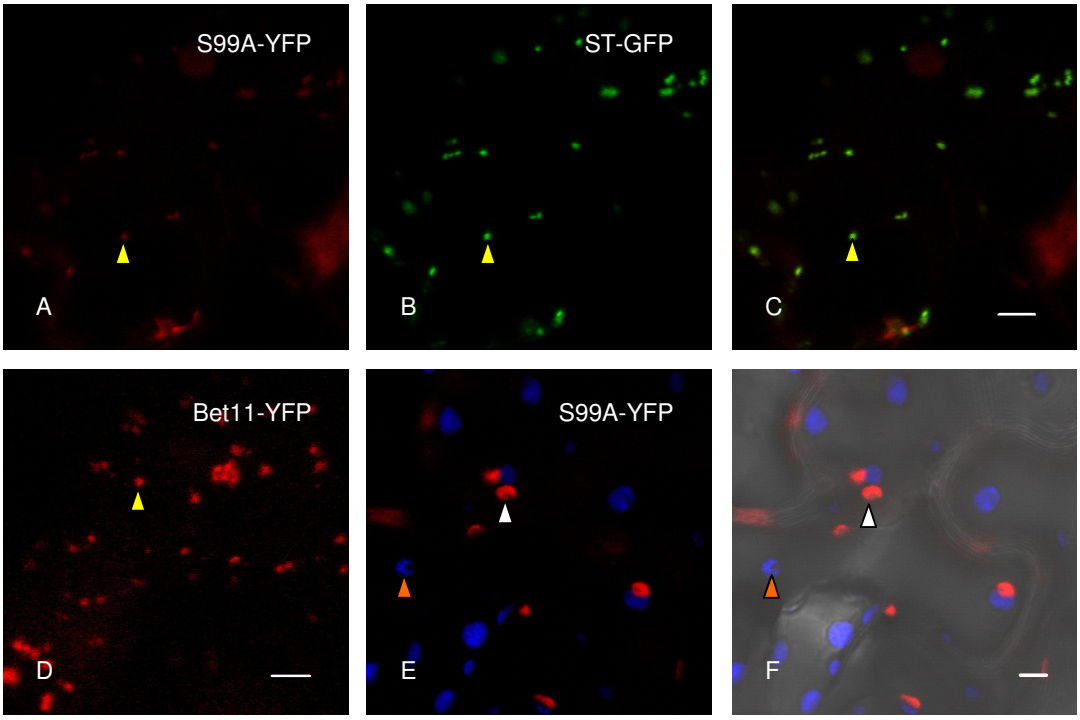

Figure 3.8 S99A-YFP formed large aggregates. Confocal images of tobacco leaf epidermal cells 3 days after the *A. tumefaciens* infiltration with S99A-YFP, Bet11-YFP and ST-GFP ($O.D._{600}$ = 0.05). The fluorescence of S99A-YFP in the Golgi stacks (yellow arrowhead) (A) was very low compared with Bet11-YFP (D). S99A-YFP formed large aggregates localized in cytosol or ER (panel E and F, white arrowheads). Using microscope settings to detect chlorophyll it was possible to distinguish the chloroplasts (orange arrowheads) from S99A-YFP aggregates. (C) Merged image of A and B. (F) Merged image of E and bright field. Scale bars 5 µm.

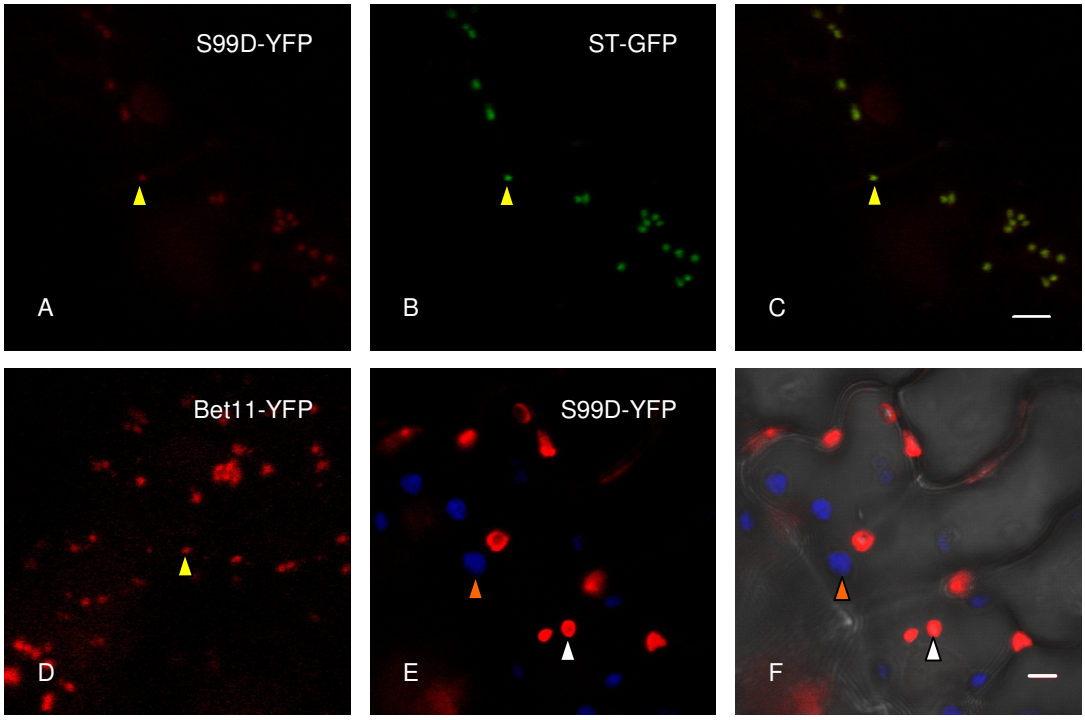

Figure 3.9 S99D-YFP formed large aggregates Confocal images of tobacco leaf epidermal cells 3 days after the *A. tumefaciens* infiltration with S99D-YFP, Bet11-YFP and ST-GFP ($O.D._{600}$ = 0.05). The fluorescence of S99D-YFP in the Golgi stacks (yellow arrowhead) (A) was very low compared with Bet11-YFP (D). S99D-YFP formed large aggregates localized in cytosol or ER (panel E and F, white arrowheads). Using microscope settings to detect chlorophyll it was possible to distinguish the chloroplasts (orange arrowheads) from S99D-YFP aggregates. (C) Merged image of A and B. (F) Merged image of E and bright field. Scale bars 5 µm.

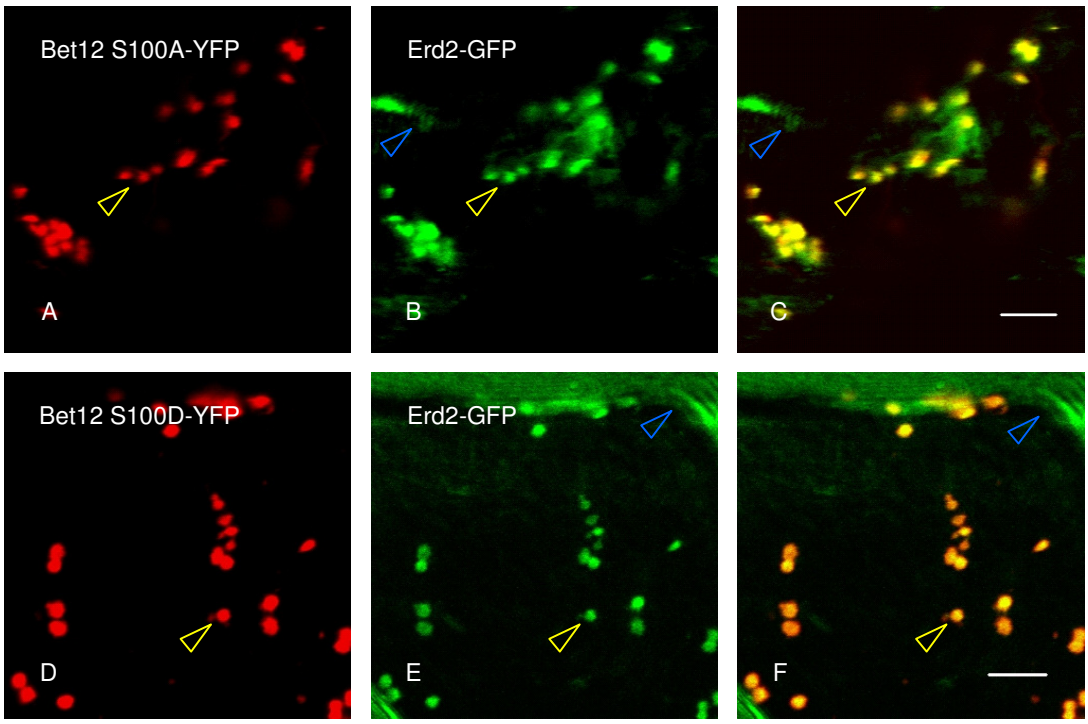

Figure 3.10 Mutations of serine 100 in Bet12 did not have an effect on Bet12 distribution. Confocal images of tobacco leaf epidermal cells 3 days after the *A. tumefaciens* infiltration with S100A-YFP, S100D-YFP ($O.D._{600}$ = 0.05) and Erd2-GFP ($O.D._{600}$ = 0.2). Bet12 mutants (A and D) co-localized on the Golgi stacks (yellow arrowheads) with Erd2-GFP (B and E). (C) Merged image of A and B. (F) Merged image of D and E. Blue arrowheads show laser reflections. Scale bars 5 µm.

3.4 Studying the function of Bet11 and Bet12 using SALK lines

To define the function of Bet11 and Bet12 in the secretory pathway, I characterized three different SALK lines, one for Bet11 (SALK_150636 with T-DNA insertion in the promoter) and two for Bet12 (SALK_150384 and SALK_129297 both of them with T-DNA insertion in the promoter). After genotyping and selection of homozygous plants for the T-DNA insertion, I investigated gene expression using RT-PCR (Figure 3.11).

Despite the T-DNA insertion, *BET12* was expressed in both SALK lines that I screened and the PCR amplification (primers LC11 and LC12; see Table 4A) product was detectable after 25 cycles both in wild type and mutant plants suggesting that the transcription level of *BET12* was comparable in wild type and mutants (Figure 3.11-B). On the other hand, the T-DNA insertion in the promoter of *BET11* in SALK_150636 leads to a down regulation of Bet11 gene transcription compared with the transcription in wild type plants. In mutant plants Bet11 gene transcript was detectable after 31 PCR cycles (primers LC9 and LC10; see Table 4A) whereas in wild type plants the transcript was detectable after only 25 cycles (Figure 3.11-A).

On the other hand, Bet11 and Bet12 are the only two members in this SNARE family and the down regulation of one member of the family could lead to the up-regulation of the other gene to compensate the knock down effects. To determine if this was the case, I have analyzed the expression of *BET12* gene in *BET11* knock-down plants (Figure 3.11-B). The expression of Bet12 in the *BET11* SALK line was comparable to wild type plants (in both cases the amplification product was detectable at 25 cycles) giving an evidence that the absence of Bet11 may not influence the transcription of *BET12*.

No obvious phenotype was detectable in these plants. Therefore, I have considered

the possibility that *BET11* is involved in a non-evident phenotype and the starting point for this investigation was the expression analysis of Bet11 in different organs and under different biotic and abiotic stresses. Using Genevestigator (https://www.genevestigator.ethz.ch) I have observed that *BET11* seems to be slightly down-regulated in presence of high concentration of CO_2, cold stress and hypoxia and it is slightly up-regulated during potassium deprivation, high concentration of mannitol, senescence, heat and osmotic stress and during flower development (Figure 3.12; *BET12* was not present in Genevestigator database). Using this information, I decided to investigate the possible role of Bet11 during osmotic stress response and pollen germination. It is known that the correct functioning of the secretory pathway is important for the development of polarized organs such as roots and pollen tubes (Campanoni and Blatt, 2007). I have followed *in vitro* and *in vivo* the germination of pollen from wild type and mutant flowers to test if the knock down of *BET11* was lethal to pollen (Figure 3.13). Nevertheless, I observed germination in both wild type and mutant pollen and this result excluded a possible role of *BET11* in pollen viability.

Using Genevestigator, I also analyzed the expression levels of *BET11* during different biotic and abiotic stresses (Figure 3.12). I decided to investigate if it was possible to find cellular evidence of salt sensitivity or tolerance in *BET11* knock-down mutants. Specifically, I focused on vacuolar morphology. The vacuole plays a fundamental role in salt tolerance by sequestering sodium (Leshem et al., 2006). The correct function of vesicle fusion with the vacuole was determined by salt stress tolerance (Leshem et al., 2006). I germinated *BET11* mutant seeds and wild type seeds on MS medium and treated the 10 day roots with 250 mM NaCl for 10 min to cause a high salinity shock (Sokol et al., 2007). To analyze the effect of salt stress on the vacuolar morphology I used

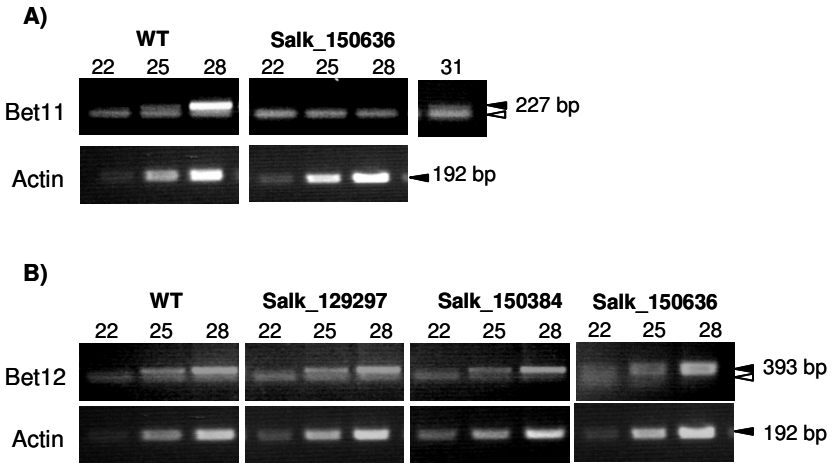

Figure 3.11 *BET11* is down-regulated in SALK_150636. A) After RT-PCR on the total mRNA extract from wild type and mutant seedlings (see Table A9 of the Appendix), *BET11* cDNA was amplified with PCR using specific primers (for PCR conditions see Tables A7 and A8 of the Appendix). To compare the expression in wild type and mutant plants, the PCR were stopped at 22, 25 and 28 cycles. A specific amplification band was detectable at 25 amplification cycles in wild type plants, which was even more evident at 28 cycles. On the contrary, in SALK_150636 a weak amplification band was detectable only after 31 cycles. As a housekeeping gene, I used actin. In panel **B)** I repeated the same experiment in Bet12 SALK lines (SALK_129297 and SALK_150384) using specific primers for *BET12*. This experiment proved that the level of expression of *BET12* in *BET12* SALK lines is comparable to wild type plants. I also tested the expression of *BET12* in the *BET11* SALK line showing that a difference in *BET12* expression between wild type and mutant plants was not detectable. Every PCR was repeated at least three times. Black arrowheads show the specific PCR products while white arrowheads show nonspecific bands.

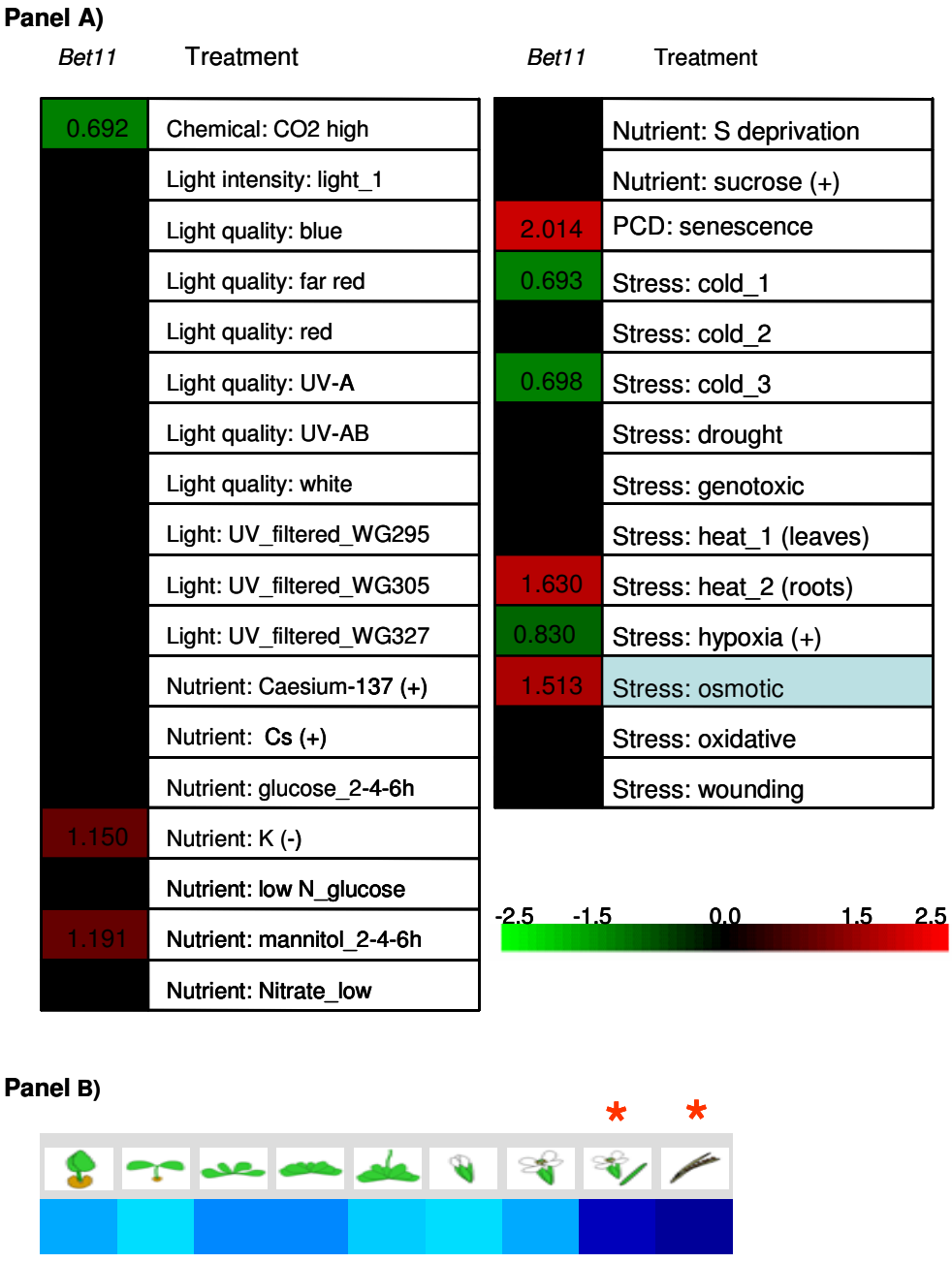

Figure 3.12 Genevestigator analysis of *BET11* expression. Panel A represents the expression of *BET11* during different abiotic stresses. Up-regulation is represented in red, down regulation in green and basal level in black. Panel B represents the expression of *BET11* during different development stage. Blue intensity is the expression index.

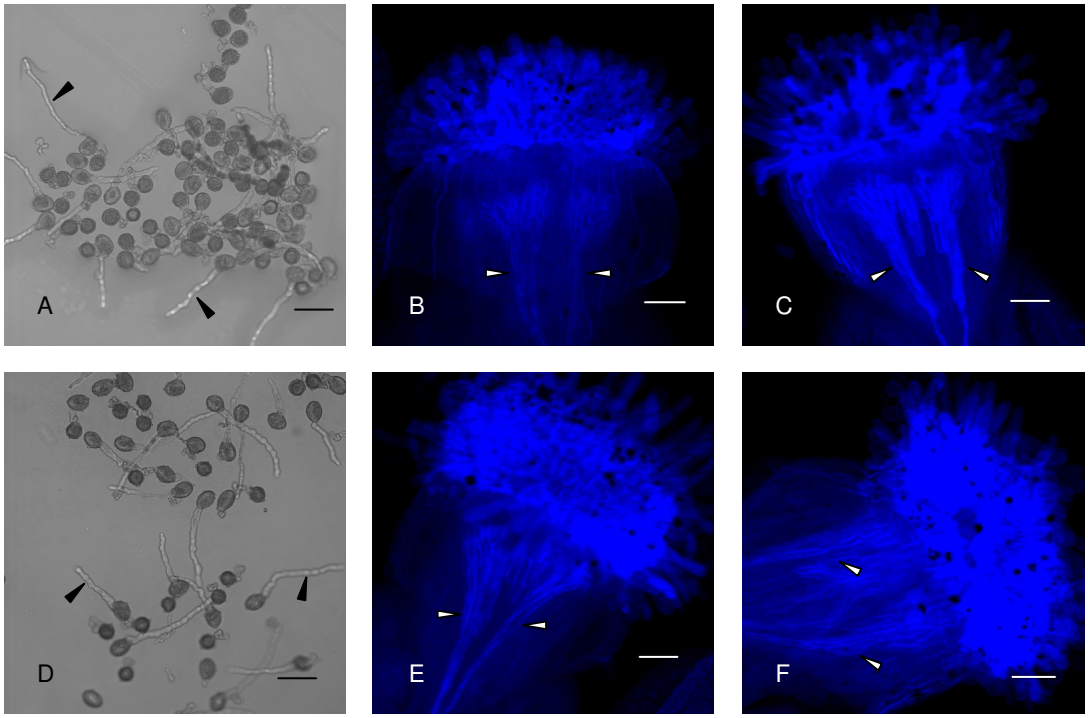

Figure 3.13 Bet11 does not influence pollen germination. Pollen grains from wild type (A) and SALK_150636 (D) plants were germinated on basic medium prepared as described by Fan et al. (2001). The germination of pollen grains was checked after 5 hour incubation and I saw germination in both wild type and mutant (black arrowheads). Panels B, C, E and F show pollen germination *in vivo*. Pistils from wild type (B and C) and mutant plants (E and F) have been stained with a solution of aniline blue (as described by Singh et al. (1992)) to visualize pollen germination (white arrowheads) and then observed with the confocal microscope. Scale bars = 50 µm

FM4-64, a lipophilic steryl dye which is known to follow the endocytic pathway from the plasma membrane via endosomes to the vacuole in various eukaryotes including plants (Ueda et al., 2001; Uemura et al., 2004; Bolte et al., 2004). After staining with FM4-64, I analyzed the vacuolar morphology using confocal microscopy. However, no significant difference between wild type and *bet11* vacuoles was detected (Figure 3.14). I also tested *bet11* mutant and wild type plants for long term salt resistance. To do this, I germinated mutant and wild type seeds to MS medium and I transferred the 4 day seedlings on MS plus 120 mM NaCl. The primary screen showed an increased salt resistance of the mutant roots that looked longer and more branched than wild type roots. Nevertheless, this difference was not constant in subsequent experiments and it was impossible to statistically compare the results. These data and the results obtained with the high salinity shock experiments suggest that the role of Bet11 may not be linked directly with salt stress tolerance.

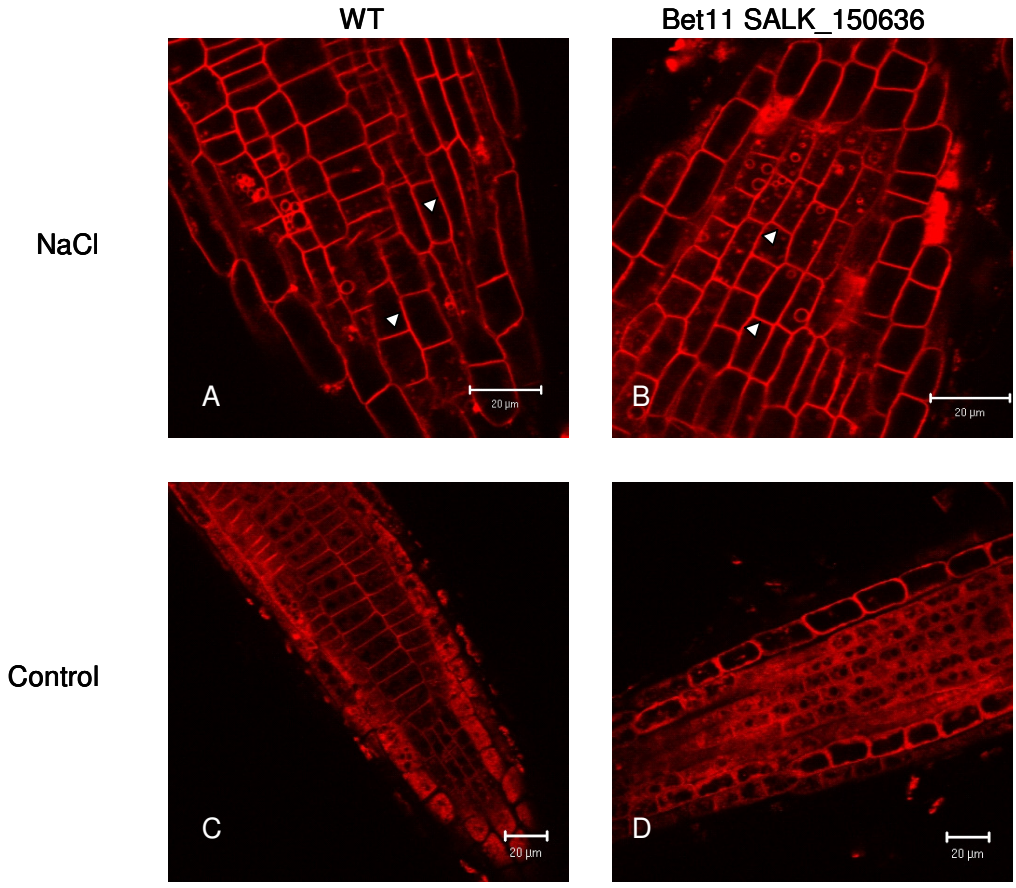

Figure 3.14 Bet11 does not influence tonoplast morphology during salt stress. 10 day old wild type (A) and mutant (B) *Arabidopsis* roots treated with 250 mM NaCl for 10 min then stained with FM 4-64 and analyzed by confocal microscopy. No significant differences were detectable. The white arrowheads in panels A and B point to the mega-vesicles that are normally observed in *Arabidopsis* roots during salt stresses (Leshem et al., 2006) Panel C and D represent the control of non-treated root from wild type and mutant seedlings respectively. White arrowheads indicate vacuoles. Scale bars = 20 µm.

4. DISCUSSION

4.1 Bet11 and Bet12 have different intracellular distribution

In the *Arabidopsis* genome there are 54 genes coding for SNAREs or putative SNAREs. The SNARE family consists of several members that share similar structures. They play a crucial role in intracellular trafficking in eukaryotic cells. It has been shown *in vitro* that a single SNARE can interact with several other SNAREs in a non-specific way (Jahn and Scheller, 2006). For this reason, the primary regulation of SNARE function *in vivo* is at the level of their intracellular distribution (Zeng et al., 2003).

Bet11 and Bet12 are two *Arabidopsis* SNAREs that share 60% amino acid sequence identity. I have demonstrated that these SNAREs have a different intracellular distribution. Bet12 is localized on the Golgi stacks. Bet11 is found in the ER, Golgi stacks and endosomes. These results suggest distinct roles for Bet11 and Bet12 within the secretory pathway of plant cells.

A similar case can be seen in Vti11 and Vti12, two other *Arabidopsis* SNAREs. Despite their high amino acid sequence identity (more than 60%), Vti11 and Vti12 have completely different localizations, in different membrane fusion steps (Surpin et al., 2003; Sanmartin et al., 2007). In particular, Vti12 is involved in trafficking to the storage vacuole and in autophagy (Surpin and Raikhel, 2004; Sanmartin et al., 2007); whereas, Vti11 is involved in trafficking to the lytic vacuole (Sanmartin et al., 2007).

4.2 Subcellular targeting of Bet11 and Bet12

It is known that the trafficking of a cargo protein in the secretory pathway is determined by its intrinsic sorting signal(s). This signal(s) can be a short peptide or a structural motif (Mancias and Goldberg 2007; Bonifacino and Glick, 2004). Relatively little information about SNARE sorting signals is available, particularly for plant SNAREs.

Studying chimaeras of these Bet11 and Bet12 I have demonstrated that the distribution of these two SNAREs to targeting organelles is the result of different sorting signals. The transmembrane region of Bet12 contains a signal that is sufficient to transport Bet12 from the ER to the Golgi stacks. On the other hand, the transmembrane region of Bet12 fused to YFP is only partially localized in the Golgi stacks. mBet12-YFP also appears in the ER. My hypothesis is that the Bet12 transmembrane region acts in synergy with the cytosolic domain to guarantee the proper localization to the Golgi stacks. Similarly, the localization of the yeast Golgi apparatus SNARE Sed5 is only partially determined by its transmembrane domain (Banfield et al., 1994; Weinberger et al., 2005) and it needs a second localization signal in the cytosolic region to properly target to the Golgi apparatus (Weinberger et al., 2005). Also in mammals, the targeting of syntaxin 3 and 4 depend on two distinct targeting signals, one in the cytosolic domain and another in the transmembrane region, which act in synergy to guarantee the correct cycling of these SNAREs between the ER and the Golgi apparatus (Bulbarelli et al., 2002).

I have also shown that the cytosolic domain and, in particular, the N-terminal region, but not the transmembrane domain, of Bet11 contains the sorting signal for correct

targeting of this SNARE. Specifically, the presence of the N-terminal region seemed essential for the proper targeting of this protein to the endosomes and, lacking the cytosolic region integrity, Bet11 caused mistargeting of secretory proteins. In this N-terminal protein domain, I have found a putative DxxxLL motif that could be important for Bet11 targeting but I was unable to identify any specific residue or amino acid sequence important for the targeting of Bet12.

These results suggest that either multiple signals or the structural conformation of the cytosolic region of these two SNAREs may be involved in their targeting and /or function. The yeast t-SNARE Sec22 (R), for example, contains two signals in the cytosolic domain that act together to drive the export of Sec22 from the ER (Mancias and Goldeberg, 2007). The first signal is an amino acid sequence that binds the COPII sub-complex Sec23/Sec24 (Mossessova et al., 2003). It has been shown that this signal is essential but not sufficient for the export of Sec22 from the ER (Liu et al., 2004; Mancias and Golberg, 2007). A second signal located within the SNARE-motif is necessary for the correct sorting. This signal is a folded epitope that can bind Sec23/Sec24 and guarantee the exit from the ER (Mancias and Goldberg, 2007). Another example of a structural motif that acts as a sorting signal is illustrated by Vamp4 and Vamp5. In mammals, Vamp4 and Vamp5 are two members of the Vamp sub-family of SNAREs involved in post-Golgi traffic. They share high identity of sequence but, like Bet11 and Bet12, they have different sub-cellular distributions: Vamp4 labels the TGN and Vamp5 is localized on the PM (Zeng et al., 2003). Studying the chimeras of these two SNAREs, Zeng et al. (2003) have demonstrated that the cytosolic region contains the sorting signal for both these proteins. Nevertheless, they did not identify a signal-peptide sequence. They have concluded that a higher order of

structural information might be involved in Vamp4 and Vamp5 sorting.

4.3 Phosphorylation of Bet11 and Bet12

A second level of SNARE activity regulation, after the control of intracellular distribution, is post-translational modification. To avoid aspecific membrane fusions, it is important that SNAREs do not interact before they reach their site of action and the SNAREs are activated only in proximity of the site of fusion (Snyder et al., 2006). In particular in mammals, it has been demonstrated that SNARE phosphorylation prevents SNARE complex assembly (Snyder et al., 2006). It is possible that phosphorylation causes a conformational change in SNARE structure that inhibits SNARE-SNARE interactions. It has also been shown that phosphorylation can influence SNARE localization (Foletti et al., 2000; Snyder et al., 2006) and interaction with SNARE regulators (Tian et al., 2003; Snyder et al., 2006).

In yeast, Weinberger et al. (2005) have shown that the t-SNARE Sed5, localized on the Golgi apparatus, is phosphorylated and this post-translational modification influences Golgi apparatus morphology and function. The phosphorylation site is a serine residue proximal to the transmembrane domain. By sequence alignment with yeast Sed5 we have identified a serine in the same position in the sequence of Bet11 (Ser99) and Bet12 (Ser100). The analysis of the serine mutant of Bet11 and Bet12 suggested that this amino acid is only important for the localization of Bet11. The mutation of Ser99 caused the formation of large aggregates of mutant protein and the reduction of Bet11 traffic to the Golgi stacks. Bioinformatic analysis proved that this residue is a putative phosphorylation site and, even though I was unable to biochemically prove the effective phosphorylation of this amino acid; I have shown that

this residue is important for the correct trafficking of Bet11, either guaranteeing correct folding of the protein or as a residue involved in post-translational modification regulatory events.

4.4 SALK line analysis

To define the role of Bet11 and Bet12 in the plant secretory pathway, I decided to analyze T-DNA insertion lines of *Arabidopsis* plants. I identified a mutant that shows down-regulation of Bet11 expression. Nevertheless, this mutant did not have an obvious phenotype and I attempted to search for a phenotype using different approaches. In fact, gene disruption may cause several different phenotypes. In particular SNAREs are involved in numerous cellular functions and a SNARE knock-out can have unexpected results. A clear example is the *Arabidopsis* t-SNARE Syp61 (Qc). Syp61 drives membrane fusion in post-Golgi traffic. Zhu et al. (2002) have shown that *Arabidopsis* plants lacking *SYP61* were more resistant to salt stresses than wild type plants. How Syp61 influences the tolerance to salt stress is still not completely understood, but it appears that this SNARE has a more complex role in cell physiology than driving membrane fusion. Since the *BET11* mutants were lacking an obvious phenotype, we decided to further investigate the possibility of a hidden phenotype. As an indicator of *BET11* expression we resorted to Genevestigator analysis. The results obtained with the bioinformatic analysis gave us the idea that Bet11 might be involved in pollen tube development and salt stress tolerance. Nevertheless, the experiments conducted to prove these hypotheses did not provide a definitive conclusion.

It is possible that Bet11 is involved in different cellular events or another SNARE complements Bet11 function. In several cases the deletion of a single SNARE can result

in unexpectedly mild phenotypes (Jahn and Scheller, 2006). For example, in neuronal cells, SNAP-25 and SNAP-23, two SNAREs involved in regulated exocytosis, can substitute for each other (Sørensen et al., 2003; Jahn and Scheller, 2006). This observation suggests that some SNAREs can functionally replace each other for certain roles. The major candidate to replace Bet11 was Bet12, the only other member of Bet family; however, I have demonstrated that expression levels of Bet12 in Bet11 mutants are comparable with wild type plants. Yeast Sec22, an R-SNARE involved in ER-Golgi stacks trafficking, can be substituted by Ykt6, an R-SNARE that acts in post-Golgi trafficking (Liu and Barlowe, 2002; Jahn and Scheller, 2006). Consequently, it is possible that a SNARE belonging to a different family and involved in a different pathway may functionally replace Bet11. This might explain the absence of an obvious phenotype in these SALK mutants.

5. CONCLUSIONS

The first objective of this thesis was the identification of linear amino acid sequence(s) or tridimensional protein motif(s) important for Bet11 and Bet12 intracellular sortings. I have shown that Bet11 and Bet12 have different intracellular distribution. By studying the localization of chimaeric proteins of Bet11 and Bet12, I can conclude that the distribution of these two SNAREs to the targeting compartments is the consequence of multiple domains. My results also indicate that positioning of these domains is not identical between the two SNAREs. In particular, evidence suggests that the intracellular distribution of Bet12 depends both on transmembrane and cytosolic domain that act in synergy to ensure the sorting of Bet12 to Golgi stacks. The intracellular sorting of Bet11 seems more complex. In the N-terminal region of Bet11 is the sorting signal for targeting of this SNARE to post-Golgi compartments but the structural modification of the cytosolic domain can cause alteration of post-Golgi trafficking.

The second objective of this thesis was to study the role of phosphorylation in Bet11 and Bet12 traffic and function. I have not biochemically demonstrated the phosphorylation of Bet11 and Bet12, but I have shown that the putative phosphorylation site on Bet11, Ser99, is important for Bet11 sorting or folding. I have also demonstrated that the same residue is not important for Bet12 traffic confirming that the sorting mechanisms of these two SNAREs are different.

The third objective was to study the role of Bet11 and Bet12 in vesicular traffic. The different intracellular distribution of Bet11 and Bet12 suggests a different role in the

secretory pathway of plant cells. In particular, the localization of Bet11 on the TGN and endosomes provides strong evidence for this SNARE's role in post-Golgi traffic.

6. APPENDIX

Table A1. Growth Media

Medium	Formulation
LB liquid	10 g/l bacto peptone-tryptone, 5 g/l yeast extract, 10 g/l NaCl
LB solid	10 g/l bacto peptone-tryptone, 5 g/l yeast extract, 10 g/l NaCl, 10 g/l agar
YT	16 g/l bacto-tryptone, 10 g/l yeast extract, 5 g/l NaCl, pH 7.0

Table A2. Solutions and Antibiotics

Solution	**Formulation**
Gentamycin	Stock solution 25 mg/ml in water
IF	20 mM $Na_3(PO_4)$, 500 mM MES, 200 mM acetosyringone, 5 mg/ml glucose
Kanamycin	Stock solution 100 mg/ml in water
Loading Buffer 10X	35% glycerol, 2.5 g/l bromophenol blue in TAE 10X
P1	1 mM EDTA, 50 mM TRIS. pH 8.0
P2	0.2 N NaOH, 1% SDS
P3	11.5% acetic acid, 3 M potassium acetate. pH 5.5
TAE 50X	2 M Tris base, 1 M glacial acetic acid, 0.1 M $Na_2EDTA_2H_2O$
TFBI	30 mM $KC_2H_3O_2$, 100 mM RbCl, 10 mM $CaCL_2$-$2H_2O$, 50 mM $MnCl_2$-$4H_2O$, 15% glycerol. pH 5.8 with 0.2 M CH_3COOH.
TFBII	10 mM MOPS, 10 mM RbCl, 75 mM $CaCl_2$-$2H_2O$, 15% glycerol. pH 6.6 with 1 M KOH
Extraction Buffer (for *Arabidopsis* genomic DNA)	200 mM Tris-HCl (pH 7.5), 250 mM NaCl, 25 mM EDTA, 0.5% SDS

Table A3. Kits and Enzymes

Kit and Enzymes	**Supplier**
QIAquick Gel Extraction Kit	Qiagen (www.qiagen.com)
QIAquick PCR Purification Kit	Qiagen (www.qiagen.com)
RNeasy Plant Mini Kit	Qiagen (www.qiagen.com)
Pfu DNA Polymerase	Fermentas (www.fermentas.com)
Ribonuclease A	Fermentas (www.fermentas.com)
SacI	NEB (www.neb.com)
SuperScript III First-Strand Synthesis SuperMix	Invitrogen (www.invitrogen.com)
T4 DNA ligase	Invitrogen (www.invitrogen.com)
XbaI	NEB (www.neb.com)
GoTaq DNA polymerase	Promega (www.promega.com)

Table A4. List of Primers used in this study

Primer	Sequence	Protein
LC9	GCTCTAGACCATGAATCCTAGAAGGGAG	Bet11
LC10	ACGCGTCGACATGGCCCGAGTAAGATAGTATAT	Bet11
LC11	GCTCTAGACCATGAACTTTCGAAGGGAGAAT	Bet12
LC12	ACGCGTCGACATGGCCCCTTTGATGTAGTTTAA	Bet12
MR1	CATGACCGTCGACTTCATTCTTCGGCTTGAC	cBet11
MR2	CATGACCGTCGACTTTTTGCAACTTTTTCGATTAG	cBet12
MR3	CATGTATGTCTCCAGATAGTCGTTTTAAGAGAATG	Bet11/12/11
MR4	AAACGACTATCTGGAGACATACATGAAGAAGTTG	Bet11/12/11
MR5	CATTTATATCGCCAGTCACTCTCTTGAGAAACG	Bet12/11/12
MR6	CAAGAGAGTGACTGGCGATATAAATGAAGAGGTCG	Bet12/11/12
MR7	CAGGACGTCTAGATGCTGACGCTCGTGGCATCGTTTG	mBet11
MR8	CAGGACGTCTAGATGCTCATAGCTTATTTTGTGCTCC	mBet12
MR21	CAGGACGTCTAGATGTGGTGGCTACTGGTTTTA	TM Sec12
MMR7	GTGTTTGAGACAAAGGCAAGCCGAAGAATGCTG	Bet11 S99A
MMR8	CAGCATTCTTCGGCTTGCCTTTGTCTCAAACAC	Bet11 S99A
MMR9	GTGTTTGAGACAAAGGACAGCCGAAGAATGCTG	Bet11 S99D
MMR10	CAGCATTCTTCGGCTGTCCTTTGTCTCAAACAC	Bet11 S99D
MMR11	GTCTTTGAGAAGAAGGCTAATCGAAAAAGTTGC	Bet12 S100A
MMR12	GCAACTTTTTCGATTAGCCTTCTTCTCAAAGAC	Bet12 S100A
MMR13	GTCTTTGAGAAGAAGGATAATCGAAAAAGTTGC	Bet12 S100D
MMR14	GCAACTTTTTCGATTATCCTTCTTCTCAAAGAC	Bet12 S100D

Table A5. Reagents for PCR using *Pfu* DNA Polymerase

Reagent	**Finale volume and concentration**
Pfu buffer 10X	20 µl (1X)
DNA template	1 µl (1-5 ng)
Pfu DNA Polymerase	1 µl (2.5 U)
dNTPs (100 mM)	4 µl (2 mM)
Primer sense (100 µmoles/µl)	0.6 µl (0.3 µM)
Primer antisense (100 µmoles/µl)	0.6 µl (0.3 µM)
H_2O	To 200 µl

Table A6. PCR amplification protocol using *Pfu* DNA Polymerase

Temperature	**Time**	**Number of cycles**
94°C	4 min	1
94°C 50-52°C 72°C	30 sec 45 sec variable	20
72°C	4 min	1

Table A7. Reagents for PCR using the GoTaq Flexi Polymerase

Reagent	**Final volume and concentration**
Green GoTaq Flexi Buffer 5X	5 µl (1X)
cDNA template	0.5 µl (<0.25 µg)
GoTaq Flexi Polymerase	0.2 µl (0.25 U)
dNTPs (100 mM)	0.5 µl (2 mM)
Primer sense (100 µmoles/µl)	0.1 µl (0.4 µM)
Primer antisense (100 µmoles/µl)	0.1 µl (0.4 µM)
$MgCl_2$ solution (25 mM)	2 µl (2 mM)
H_2O	To 25 µl

Table A8. PCR amplification protocol using the GoTaq Flexi Polymerase

Temperature	**Time**	**Number of cycles**
94°C	2 min	1
94°C 55°C 72°C	30 sec 45 sec variable	variable
72°C	5 min	1

Table A.9 RT-PCR reagents and amplification protocol

Reagent	**Final volume and concentration**
Up to 5 µg total RNA	n µl
Oligo(dT)$_{20}$ (50 µM)	1 µl (6,25 µM)
Annealing Buffer	1 µl
RNase/DNase-free water	To 8 µl

This mix was incubated at 65°C for 5 min and then place on ice for at least 1 minute. At the tube was added:

Reagent	**Final volume and concentration**
First-Strand Reaction Mix (2X)	10 µl (1X)
SuperScriptIII/RNaseOUT Enzyme Mix	2 µl

This mix was incubated 50 min at 50°C.

7. REFERENCES

Altan-Bonnet N, Sougrat R, Lippincott-Schwartz J. (2004). Molecular basis for Golgi maintenance and biogenesis. Curr. Opin. Cell Biol. **16**, 364-72.

Antonny B, Bigay J, Casella JF, Drin G, Mesmin B, Gounon P. (2005). Membrane curvature and the control of GTP hydrolysis in Arf1 during COPI vesicle formation. Biochem. Soc. Trans. **33**, 619-22.

Arien H, Wiser O, Arkin IT, Leonov H, Atlas D. (2003). Syntaxin 1A modulates the voltage-gated L-type calcium channel (Ca(v)1.2) in a cooperative manner. J. Biol. Chem. **278**, 29231-9.

Banfield DK, Lewis MJ, Rabouille C, Warren G, Pelham HR. (1994). Localization of Sed5, a putative vesicle targeting molecule, to the cis-Golgi network involves both its transmembrane and cytoplasmic domains. J. Cell Biol. **127,** 357-71.

Barlowe C. (1995). COPII: a membrane coat that forms endoplasmic reticulum-derived vesicles. FEBS Lett. **369**, 93-6.

Batoko H, Zheng HQ, Hawes C, Moore I. (2000). A rab1 GTPase is required for transport between the endoplasmic reticulum and golgi apparatus and for normal golgi movement in plants. Plant Cell. **12**, 2201-18.

Boevink P, Oparka K, Santa Cruz S, Martin B, Betteridge A, Hawes C. (1998). Stacks on tracks: the plant Golgi apparatus traffics on an actin/ER network. Plant J. **15**, 441-7.

Bolte S, Talbot C, Boutte Y, Catrice O, Read ND, Satiat-Jeunemaitre B. (2004). FM-dyes as experimental probes for dissecting vesicle trafficking in living plant cells. J. Microsc. **214**, 159-73.

Bonifacino JS, Glick BS. (2004). The mechanisms of vesicle budding and fusion. Cell **116**, 153-66.

Brandizzi F, Irons SL, Johansen J, Kotzer A, Neumann U. (2004). GFP is the way to glow: bioimaging of the plant endomembrane system. J. Microscopy 214, 138-158.

Bulbarelli A, Sprocati T, Barberi M, Pedrazzini E, Borgese N. (2002).Trafficking of tail-anchored proteins: transport from the endoplasmic reticulum to the plasma membrane and sorting between surface domains in polarised epithelial cells. J. Cell Sci. **115**, 1689-702.

Cai H, Reinisch K and Ferro-Novick S. (2008). Coats, Tethers, Rabs, and SNAREs Work Together to Mediate the Intracellular Destination of a Transport Vesicle. J. Dev. Cell **12,** 671-682.

Campanoni P, Blatt MR. (2007). Membrane trafficking and polar growth in root hairs and pollen tubes. J. Exp. Bot. **58**, 65-74.

Chalfie M, Tu Y, Euskirchen G, Ward WW, Prasher DC. (1994). Green fluorescent protein as a marker for gene expression. Science **263**, 802-5.

Chatre L, Brandizzi F, Hocquellet A, Hawes C, Moreau P. (2005). Sec22 and Memb11 are v-SNAREs of the anterograde endoplasmic reticulum-Golgi pathway in tobacco leaf epidermal cells. Plant Physiol. 139, 1244-54.

Chen YA, Scheller RH. (2001). SNARE-mediated membrane fusion. Nat. Rev. Mol. Cell Biol. **2**, 98-106.

Collins NC, Thordal-Christensen H, Lipka V, Bau S, Kombrink E, Qiu JL, Hückelhoven R, Stein M, Freialdenhoven A, Somerville SC, Schulze-Lefert P. (2003). SNARE-protein-mediated disease resistance at the plant cell wall. Nature 425, 973-7.

Conibear E, Cleck JN, Stevens TH. (2003). Vps51p mediates the association of the GARP (Vps52/53/54) complex with the late Golgi t-SNARE Tlg1p. Mol. Biol. Cell **14**, 1610-23.

Cormet-Boyaka E, Jablonsky M, Naren AP, Jackson PL, Muccio DD, Kirk KL. (2004). Rescuing cystic fibrosis transmembrane conductance regulator (CFTR)-processing mutants by transcomplementation. Proc. Natl. Acad. Sci. USA **101**, 8221-6.

daSilva LL, Snapp EL, Denecke J, Lippincott-Schwartz J, Hawes C, Brandizzi F. (2004). Endoplasmic reticulum export sites and Golgi bodies behave as single mobile secretory units in plant cells. Plant Cell **16,** 1753-71.

De Matteis MA, Luini A. (2008). Exiting the Golgi complex. Nat. Rev. Mol. Cell Biol. **9**, 273-84.

Dhonukshe P, Aniento F, Hwang I, Robinson DG, Mravec J, Stierhof YD, Friml J. (2007). Clathrin-mediated constitutive endocytosis of PIN auxin efflux carriers in Arabidopsis. Curr. Biol. **17**, 520-7.

Dulhanty AM, Riordan JR. (1994). Phosphorylation by cAMP-dependent protein kinase causes a conformational change in the R domain of the cystic fibrosis transmembrane conductance regulator. Biochemistry **33**, 4072-9.

Elazar Z, Scherz-Shouval R, Shorer H. (2003). Involvement of LMA1 and GATE-16 family members in intracellular membrane dynamics. Biochim. Biophys. Acta. **1641**, 145-56.

Fan LM, Wang YF, Wang H, Wu WH. (2001). In vitro Arabidopsis pollen germination and characterization of the inward potassium currents in Arabidopsis pollen grain protoplasts. J. Exp. Bot. **52**, 1603-14.

Fasshauer D. (2003). Structural insights into the SNARE mechanism. Biochim. Biophys. Acta. **1641**, 87-97.

Fasshauer D, Sutton RB, Brunger AT, Jahn R. (1998) Conserved structural features of the synaptic fusion complex: SNARE proteins reclassified as Q- and R SNAREs. Proc. Natl. Acad. Sci. USA **95**,15781–15786.

Foletti DL, Lin R, Finley MA, Scheller RH. (2000). Phosphorylated syntaxin 1 is localized to discrete domains along a subset of axons. J. Neurosci. **20**, 4535-44.

Gerst JE. (2003). SNARE regulators: matchmakers and matchbreakers. Biochim. Biophys. Acta. **1641**, 99-110.

Hanson PI, Whiteheart SW. (2005). AAA+ proteins: have engine, will work. Nat Rev Mol. Cell Biol. **6**, 519-29.

Hanton SL, Bortolotti LE, Renna L, Stefano G, Brandizzi F. (2005).Crossing the divide--transport between the endoplasmic reticulum and Golgi apparatus in plants. Traffic. **6**, 267-77.

Hanton SL, Chatre L, Matheson LA, Rossi M, Held MA, Brandizzi F. (2008). Plant Sar1 isoforms with near-identical protein sequences exhibit different localisations and effects on secretion. Plant Mol. Biol. **67**, 283-94.

Hanton SL, Chatre L, Renna L, Matheson LA, Brandizzi F. (2007). De novo formation of plant endoplasmic reticulum export sites is membrane cargo induced and signal mediated. Plant Physiol. **143**, 1640-50.

Hanton SL, Matheson LA, Chatre L, Brandizzi F. (2009). Dynamic organization of COPII coat proteins at endoplasmic reticulum export sites in plant cells. Plant J. **57**, 963-74.

Hasegawa H, Zinsser S, Rhee Y, Vik-Mo EO, Davanger S, Hay JC. (2003). Mammalian ykt6 is a neuronal SNARE targeted to a specialized compartment by its profilin-like amino terminal domain. Mol. Biol. Cell. **14**, 698-720.

Haseloff J, Siemering KR, Prasher DC, Hodge S. (1997). Removal of a cryptic intron and subcellular localization of green fluorescent protein are required to mark transgenic Arabidopsis plants brightly. Proc. Natl. Acad. Sci. USA **18**, 2122-7.

Hawes C, Osterrieder A, Hummel E, Sparkes I. (2008). The plant ER-Golgi interface. Traffic **9**, 1571-80.

Hay JC, Klumperman J, Oorschot V, Steegmaier M, Kuo CS, Scheller RH. (1998). Localization, dynamics, and protein interactions reveal distinct roles for ER and Golgi SNAREs. J. Cell Biol. **141**, 1489-502.

Hillmer S, Movafeghi A, Robinson DG, Hinz G. (2001). Vacuolar storage proteins are sorted in the cis-cisternae of the pea cotyledon Golgi apparatus. J. Cell Biol. **152**, 41-50.

Hohl I, Robinson DG, Chrispeels MJ, Hinz G. (1996). Transport of storage proteins to the vacuole is mediated by vesicles without a clathrin coat. J. Cell Sci. **109**, 2539-50.

Hunter T. (1995). Protein kinases and phosphatases: the yin and yang of protein phosphorylation and signaling. Cell **80**, 225-36.

Jahn R, Grubmuller H. (2002). Membrane fusion. Curr Opin Cell Biol. **14**, 488-95.

Jahn R, Scheller R. (2006). SNAREs--engines for membrane fusion. Nature Reviews **7**, 631-643.

Ji J, Tsuk S, Salapatek AM, Huang X, Chikvashvili D, Pasyk EA, Kang Y, Sheu L, Tsushima R, Diamant N, Trimble WS, Lotan I, Gaisano HY. (2002). The 25-kDa synaptosome-associated protein (SNAP-25) binds and inhibits delayed rectifier potassium channels in secretory cells. J. Biol. Chem. **277**, 20195-204.

Joglekar AP, Xu D, Rigotti DJ, Fairman R, Hay JC. (2003). The SNARE motif contributes to rbet1 intracellular targeting and dynamics independently of SNARE interaction. J. Biol. Chem. **278**, 14121-14133.

Jurgens G. (2004). Membrane trafficking in plants. Annu. Rev. Cell Dev. Biol. **20,** 481-504.

Kapila J, de Rycke R, Van Montagu M, Angenon G. (1997). An *Agrobacterium* mediated transient gene expression system for intact leaves. Plant Sci. **122**, 101-108.

Kato T, Morita MT, Fukaki H, Yamauchi Y, Uehara M, Niihama M, Tasaka M. (2002). SGR2, a phospholipase-like protein, and ZIG/SGR4, a SNARE, are involved in the shoot gravitropism of Arabidopsis. Plant Cell **14**, 33-46.

Kipnis P, Thomas N, Ovalle R, Lipke PN. (2004). The ER-Golgi v-SNARE Bet1p is required for cross-linking alpha-agglutinin to the cell wall in yeast. Microbiology **150**, 3219-28.

Kreft M, Potokar M, Stenovec M, Pangrsic T, Zorec R. (2009) Regulated exocytosis and vesicle trafficking in astrocytes. Ann. N. Y. Acad. Sci. **1152**, 30-42.

Lam SK, Tse YC, Robinson DG, Jiang L. (2007). Tracking down the elusive early endosome. Trends Plant Sci. **12**, 497-505.

Lang T, Jahn R. (2008). Core proteins of the secretory machinery. Handb. Exp. Pharmacol. **184**, 107-27.

Leshem Y, Melamed-Book N, Cagnac O, Ronen G, Nishri Y, Solomon M, Cohen G, Levine A. (2006). Suppression of Arabidopsis vesicle-SNARE expression inhibited fusion of H2O2-containing vesicles with tonoplast and increased salt tolerance. Proc. Natl. Acad. Sci. USA **103**, 18008-13.

Letourneur F, Gaynor EC, Hennecke S, Démollière C, Duden R, Emr SD, Riezman H, Cosson P. (1994). Coatomer is essential for retrieval of dilysine-tagged proteins to the endoplasmic reticulum. Cell **79**, 1199-207.

Lewis MJ, Nichols BJ, Prescianotto-Baschong C, Riezman H, Pelham HR. (2000). Specific retrieval of the exocytic SNARE Snc1p from early yeast endosomes. Mol. Biol. Cell **11**, 23-38.

Liu Y, Barlowe C. (2002). Analysis of Sec22p in endoplasmic reticulum/Golgi transport reveals cellular redundancy in SNARE protein function. Mol. Biol. Cell **13**, 3314-24.

Liu Y, Flanagan JJ, Barlowe C. (2004). Sec22p export from the endoplasmic reticulum is independent of SNARE pairing. J. Biol. Chem. **279**, 27225-32.

Marash M, Gerst JE. (2001). t-SNARE dephosphorylation promotes SNARE assembly and exocytosis in yeast. EMBO J. **20**, 411-21.

Matheson LA, Hanton SL, Brandizzi F. (2006). Traffic between the plant endoplasmic reticulum and Golgi apparatus: to the Golgi and beyond. Curr. Opin. Plant Biol. **9**, 601-9.

Matheson LA, Hanton SL, Rossi M, Latijnhouwers M, Stefano G, Renna L, Brandizzi F. (2007). Multiple roles of ADP-ribosylation factor 1 in plant cells include spatially regulated recruitment of coatomer and elements of the Golgi matrix. Plant Physiol. **143**, 1615-27.

McNew JA. (2008). Regulation of SNARE-mediated membrane fusion during exocytosis. Chem. Rev. **108**, 1669-86.

Mellman, I. (1996). Endocytosis and molecular sorting. Annu. Rev. Cell Dev. Biol. **12**, 575–625.

Miller SE, Collins BM, McCoy AJ, Robinson MS, Owen DJ. (2007). A SNARE-adaptor interaction is a new mode of cargo recognition in clathrin-coated vesicles. Nature **450**, 570-4.

Mossessova E, Bickford LC, Goldberg J. (2003). SNARE selectivity of the COPII coat. Cell **114,** 483-95.

Nakano A. (2004). Yeast Golgi apparatus--dynamics and sorting. Cell Mol. Life Sci. **61**, 186-91.

Nakatsu F, Ohno H. (2003). Adaptor protein complexes as the key regulators of protein sorting in the post-Golgi network. Cell Struct. Funct. **28**, 419-29.

Newman AP, Ferro-Novick S. (1987). Characterization of new mutants in the early part of the yeast secretory pathway isolated by a [3H]mannose suicide selection. J. Cell Biol. **105**, 1587-94.

Otegui MS, Herder R, Schulze J, Jung R, Staehelin LA. (2006). The proteolytic processing of seed storage proteins in Arabidopsis embryo cells starts in the multivesicular bodies. Plant Cell **18,** 2567–2581.

Paddock SW. (2000). Principles and practices of laser scanning confocal microscopy. Mol. Biotechnol. **16**, 127-49.

Palade G. (1975). Intracellular aspects of the process of protein synthesis. Science **189**, 347-358.

Parlati F, McNew JA, Fukuda R, Miller R, Söllner TH, Rothman JE. (2000). Topological restriction of SNARE-dependent membrane fusion. Nature **407**, 194-8.

Paul MJ, Frigerio L. (2007).Coated vesicles in plant cells. Semin. Cell Dev. Biol. **18**, 471-8.

Pearse, BM. (1975). Coated vesicles from pig brain: purification and biochemical characterization. J. Mol. Biol. **97**, 93–98.

Polishchuk RS, Mironov AA. (2004). Structural aspects of Golgi function. Cell Mol. Life Sci. **61**, 146-58.

Pratelli R, Sutter JU, Blatt MR. (2004). A new catch in the SNARE. Trends Plant Sci. **9**, 187-95.

Rein U, Andag U, Duden R, Schmitt HD, Spang A. (2002). ARF-GAP mediated interaction between the ER-Golgi v-SNAREs and the COPI coat. J. Cell. Biol. **157**, 395-404.

Renna L, Hanton SL, Stefano G, Bortolotti L, Misra V, Brandizzi F. (2005). Identification and characterization of AtCASP, a plant transmembrane Golgi matrix protein. Plant Mol. Biol. **58**, 109-22.

Robinson DG, Hinz G, Holstein SE. (1998). The molecular characterization of transport vesicles, Plant Mol. Biol. **38**, 49–76.

Sallese M, Pulvirenti T, Luini A. (2006). The physiology of membrane transport and endomembrane-based signalling. EMBO J. **25**, 2663-73.

Sambrook, J, Fritsch, EF, Maniatis T. (1989). Molecular Cloning: A Laboratory Manual. (Cold Spring Harbor, NY: Cold Spring Harbor Press).

Sanderfoot AA, Assaad FF, Raikhel NV. (2000). The Arabidopsis genome: an abundance of SNAREs. Plant Physiol. **124**, 1558-1569.

Sanmartín M, Ordóñez A, Sohn EJ, Robert S, Sánchez-Serrano JJ, Surpin MA, Raikhel NV, Rojo E. (2007). Divergent functions of VTI12 and VTI11 in trafficking to storage and lytic vacuoles in Arabidopsis. Proc. Natl. Acad. Sci. USA **104**, 3645-50.

Sannerud R, Saraste J, Goud B. (2003). Retrograde traffic in the biosynthetic-secretory route: pathways and machinery. Curr. Opin. Cell Biol. **15**, 438-45.

Shimomura O, Johnson FH, SaugaY. (1962). Extraction, purification and properties of aequorin, a bioluminescent protein from the luminous hydromedusan, Aequorea. J. Cell Comp. Physiol. **59**, 223-39.

Singh A, Evensen KB, Kao TH. (1992). Ethylene Synthesis and Floral Senescence following Compatible and Incompatible Pollinations in Petunia inflata. Plant Physiol. **99**, 38-45.

Siniossoglou S, Pelham HR. (2001). An effector of Ypt6p binds the SNARE Tlg1p and mediates selective fusion of vesicles with late Golgi membranes. EMBO J. **20**, 5991-8.

Snyder DA, Kelly ML, Woodbury DJ. (2006). SNARE complex regulation by phosphorylation. Cell Biochem. Biophys. **45**, 111-23.

Sokol A, Kwiatkowska A, Jerzmanowski A, Prymakowska-Bosak M. (2007). Up-regulation of stress-inducible genes in tobacco and Arabidopsis cells in response to abiotic stresses and ABA treatment correlates with dynamic changes in histone H3 and H4 modifications .Planta **227**, 245-54.

Söllner T, Whiteheart SW, Brunner M, Erdjument-Bromage H, Geromanos S, Tempst P, Rothman JE. (1993). SNAP receptors implicated in vesicle targeting and fusion. Nature **362**, 318-24.

Sørensen JB, Nagy G, Varoqueaux F, Nehring RB, Brose N, Wilson MC, Neher E. (2003). Differential control of the releasable vesicle pools by SNAP-25 splice variants and SNAP-23. Cell **114**, 75-86.

Springer S, Schekman R. (1998). Nucleation of COPII vesicular coat complex by endoplasmic reticulum to Golgi vesicle SNAREs. Science **281**, 698-700.

Springer, S, Spang, A, Schekman, R. (1999). A primer on vesicle budding. Cell **97**, 145–148.

Stefano G, Renna L, Hanton SL, Chatre L, Haas TA, Brandizzi F. (2006a). ARL1 plays a role in the binding of the GRIP domain of a peripheral matrix protein to the Golgi apparatus in plant cells. Plant Mol. Biol. **61**, 431-49.

Stefano G, Renna L, Chatre L, Hanton SL, Moreau P, Hawes C, Brandizzi F. (2006b). In tobacco leaf epidermal cells, the integrity of protein export from the endoplasmic reticulum and of ER export sites depends on active COPI machinery. Plant J. **46,** 95-110.

Surpin M, Raikhel N. (2004). Traffic jams affect plant development and signal transduction. Nat. Rev. Mol. Cell Biol. **5**, 100-9.

Surpin M, Zheng H, Morita MT, Saito C, Avila E, Blakeslee JJ, Bandyopadhyay A, Kovaleva V, Carter D, Murphy A, Tasaka M, Raikhel N. (2003). The VTI family of SNARE proteins is necessary for plant viability and mediates different protein transport pathways. Plant Cell. **15**, 2885-99.

Tai WC, Banfield DK. (2001). AtBS14a and AtBS14b, two Bet1/Sft1-like SNAREs from Arabidopsis thaliana that complement mutations in the yeast SFT1 gene. FEBS Lett. **6**, 177-82.

Tian JH, Das S, Sheng ZH. (2003). Ca2+-dependent phosphorylation of syntaxin-1A by the death-associated protein (DAP) kinase regulates its interaction with Munc18. J. Biol. Chem. **278**, 26265-74.

Ueda T, Uemura T, Sato MH, Nakano A. (2004). Functional differentiation of endosomes in Arabidopsis cells. Plant J. **40**, 783-9.

Uemura T, Ueda T, Ohniwa RL, Nakano A, Takeyasu K, Sato MH. (2004) Systematic analysis of SNARE molecules in Arabidopsis: dissection of the post-Golgi network in plant cells. Cell Struct. Funct. **29**, 49-65.

Vitale A, Boston RS. (2008). Endoplasmic reticulum quality control and the unfolded protein response: insights from plants. Traffic **9**, 1581-8.

Watson RT, Pessin JE. (2001). Transmembrane domain length determines intracellular membrane compartment localization of syntaxins 3, 4, and 5. Am. J. Physiol.

Cell Physiol. **281**, C215-23.

Weber T, Zemelman BV, McNew JA, Westermann B, Gmachl M, Parlati F, Sollner TH, Rothman JE. (1998). SNAREpins: minimal machinery for membrane fusion. Cell **20**, 759-72.

Weinberger A, Kamena F, Kama R, Spang A, Gerst JE. (2005). Control of Golgi morphology and function by Sed5 t-SNARE phosphorylation. Mol. Biol. Cell **16**, 4918-30.

Xu D, Joglekar AP, Williams AL, Hay JC. (2000). Subunit structure of a mammalian ER/Golgi SNARE complex. J Biol Chem. **275**, 39631-9.

Zeng Q, Tran TT, Tan HX, Hong W. (2003). The cytoplasmic domain of Vamp4 and Vamp5 is responsible for their correct subcellular targeting: the N-terminal extenSion of VAMP4 contains a dominant autonomous targeting signal for the trans-Golgi network. J. Biol. Chem. **278**, 23046-54.

Zhang T, Hong W. (2001). Ykt6 forms a SNARE complex with syntaxin 5, GS28, and Bet1 and participates in a late stage in endoplasmic reticulum-Golgi transport. J Biol Chem. **276**, 27480-7.

Zhang T, Wong SH, Tang BL, Xu Y, Peter F, Subramaniam VN, Hong W. (1997). The mammalian protein (rbet1) homologous to yeast Bet1p is primarily associated with the pre-Golgi intermediate compartment and is involved in vesicular transport from the endoplasmic reticulum to the Golgi apparatus. J. Cell Biol. **139**, 1157-68.

Zhu J, Gong Z, Zhang C, Song CP, Damsz B, Inan G, Koiwa H, Zhu JK, Hasegawa PM, Bressan RA. (2002). OSM1/SYP61: a syntaxin protein in Arabidopsis controls abscisic acid-mediated and non-abscisic acid-mediated responses to abiotic stress. Plant Cell **14**, 3009-28.